processes

MDPI

Article

Microbial Biomass in Mesophilic and Thermophilic High-Rate Biodigestion of Sugarcane Vinasse: Similar in Quantity, Different in Composition

Lucas Tadeu Fuess [1,2,*], Matheus Neves de Araujo [1], Flávia Talarico Saia [3], Gustavo Bueno Gregoracci [3], Marcelo Zaiat [1] and Piet N. L. Lens [2]

[1] Biological Processes Laboratory, São Carlos School of Engineering, University of São Paulo, Av. João Dagnone 1100, Santa Angelina, São Carlos 13563-120, São Paulo, Brazil; matheusnevesaraujo@usp.br (M.N.d.A.); zaiat@sc.usp.br (M.Z.)
[2] National University of Ireland Galway, University Rd, Galway, H91 TK33 Galway, Ireland; piet.lens@universityofgalway.ie
[3] Institute of Marine Sciences, Federal University of São Paulo, Av. Dr. Carvalho de Mendonça 144, Encruzilhada, Santos 11070-102, São Paulo, Brazil; ft.saia@unifesp.br (F.T.S.); gregoracci@unifesp.br (G.B.G.)
* Correspondence: lt.fuess@usp.br; Tel.: +55-16-3373-8363

Abstract: This study compared the behavior of the biomass in two fixed-film anaerobic reactors operated under equivalent organic loading rates but at different temperatures, i.e., 30 °C (RMM) and 55 °C (RMT). The reactors were fed with sugarcane vinasse and molasses (both fermented) in a simulation of sequential periods of season and off-season. The dynamics of biomass growth and retention, as well as the microbial composition, were assessed throughout 171 days of continuous operation, coupled with an additional 10-day test assessing the microbial activity in the bed region. Despite the different inoculum sources used (mesophilic granular vs. thermophilic flocculent sludge types), the biomass growth yield was identical (0.036–0.038 g VSS g^{-1}COD) in both systems. The retention rates (higher in RMT) were regulated according to the initial amount of biomass provided in the inoculation, resulting in similar amounts of total retained biomass (46.8 vs. 43.3 g VSS in RMT and RMM) and biomass distribution patterns (30–35% in the feeding zone) at the end of the operation. Meanwhile, hydrogenotrophic methanogenesis mediated by *Methanothermobacter* coupled to syntrophic acetate oxidation prevailed in RMT, while the *Methanosaeta*-mediated acetoclastic pathway occurred in RMM. The results show that different anaerobic consortia can behave similarly in quantitative terms when subjected to equivalent organic loads, regardless of the prevailing methane-producing pathway. The community grows and reaches a balance (or a given cell activity level) defined by the amount of substrate available for conversion. In other words, while the metabolic pathway may differ, the endpoint (the amount of biomass) remains the same if operational stability is maintained.

Keywords: vinasse management; two-stage biodigestion; AnSTBR; biomass growth yield; specific organic loading rate; 16S rRNA gene amplicon sequencing

Citation: Fuess, L.T.; de Araujo, M.N.; Saia, F.T.; Gregoracci, G.B.; Zaiat, M.; Lens, P.N.L. Microbial Biomass in Mesophilic and Thermophilic High-Rate Biodigestion of Sugarcane Vinasse: Similar in Quantity, Different in Composition. *Processes* **2024**, *12*, 1356. https://doi.org/10.3390/pr12071356

Academic Editor: Francesca Raganati

Received: 11 June 2024
Revised: 20 June 2024
Accepted: 21 June 2024
Published: 29 June 2024

1. Introduction

Sugarcane biorefineries are designed to have a highly efficient management of thermal energy, which enables the use of waste heat in numerous applications within the processing chain. For instance, the vinasse stream released at high temperatures (85–90 °C) [1] from distillation columns can be used to heat the broth prior to fermentation. This characteristic is of particular interest to anaerobic digestion (AD) systems because different levels of temperature can be "naturally" maintained in the reactors without requiring extra energy inputs to cool down or heat up vinasse. A malleable, wide spectrum of temperatures within the mesophilic, thermophilic, and even hyperthermophilic ranges can, therefore, be implemented.

Successful results on both the mesophilic [2–4] and thermophilic [5,6] AD of sugarcane vinasse are available in the literature. Defining the processing temperature depends on several factors, with the availability of sludge to be used for reactor inoculation playing a key role. Finding mesophilic sludge sources on a large scale is easier than finding thermophilic ones, which tends to favor choosing lower AD temperatures. Mesophilic sludge sources can be enriched with thermophiles; however, this procedure depends on a careful (eventually long-term) acclimatization strategy to prevent process failure [7]. The layout of the AD plant also impacts the selection of the operating temperature. Recent studies dealing with the two-stage AD of vinasse demonstrated that high temperatures, i.e., thermophilic (55 °C) [8,9] and hyperthermophilic (70 °C) [10] conditions, favor the production of biohydrogen in the fermentative step, which facilitates or stimulates maintaining the second stage (methanogenic) unit equally at high temperatures. The establishment of sulfate reduction in the fermentation of vinasse has also been demonstrated to be favored under thermophilic (55 °C) conditions [1].

Regardless of the potential for achieving similar treatment performances, i.e., high organic matter removal rates and efficient methane production, using different operating temperatures in AD systems will produce microbial communities with (very) different characteristics, impacting both the cell growth patterns (biomass quantity) and the composition of the microbial populations (qualitative aspects). With respect to quantitative aspects, despite the higher cell growth rates (excluding cell decay) of thermophiles, mesophiles have higher net growth rates (including cell decay). The occurrence of cell lysis is enhanced at higher temperatures, conditions in which the energy requirements for cell maintenance are also increased [11,12]. High temperatures also modify (increase) the permeability of cell membranes, which can facilitate the intake of toxic compounds [13]. These harsh environmental conditions increase the cell decay rates of thermophiles [11], which may be high enough to result in lower net growth rates relative to mesophiles. In practical aspects, biomass retention levels may be higher in mesophilic reactors than in thermophilic ones if both are operated under equivalent conditions of organic loading rate (OLR) and hydraulic retention time (HRT).

In the case of microbial community composition, higher richness and diversity indices are usually observed in mesophilic systems [14] because the harsher (more extreme) the environment, the fewer microbes present with efficient metabolic mechanisms that allow their survival. For instance, an effective signalization mechanism regulates the transcription of heat-shock proteins that directly participate in protein folding by preventing denaturation events in heat shocks and also rescues or even degrades denatured structures [12,15,16]. High microbial diversity tends to provide a high functional redundancy in the microbial community, i.e., the number of microbial groups performing the same metabolic function is expected to be high [17], increasing the robustness of the system during periods of instability.

This study innovatively assessed the quantitative and qualitative characteristics of the microbial biomass in two second-stage methanogenic fixed-film reactors processing sugarcane vinasse operated under different temperature levels, namely, mesophilic (30 °C) and thermophilic (55 °C) conditions. Sequential periods of season, off-season, and season were simulated by feeding the reactors with vinasse, molasses, and vinasse to maintain continuous high-rate biogas production in sugarcane biorefineries. The biomass retention and growth patterns were compared, in addition to the microbial community characterization, using 16S rRNA gene amplicon sequencing. In particular, the impacts of replacing fermented vinasse with fermented molasses on the microbial community structure were innovatively unraveled. This study provides a deeper assessment of the reactors' performance through the analysis of specific parameters as a function of the amount of biomass, which effectively differentiates the conversion capacity of microbial communities.

2. Materials and Methods

2.1. Fixed-Film Reactors and Fermented Substrates

The two fixed-film reactors consisted of bench-scale (working volumes of 2.0 L) upflow anaerobic structured-bed reactor (AnSTBR) systems filled with polyurethane (PU) strips vertically arranged as the support material. Figure 1 shows details of the AnSTBR systems. Each reactor was subjected to a different temperature level, namely, 30 °C (RMM) and 55 °C (RMT), which required the use of different sludge sources in the inoculation step: granular sludge from a mesophilic upflow anaerobic sludge blanket (UASB) reactor processing poultry slaughterhouse wastewater (inoculation of RMM) and flocculent sludge from a thermophilic UASB processing sugarcane vinasse (inoculation of RMT)—both operated at full scale. Equivalent operating conditions (HRT and OLR) were applied to RMT and RMM for 171 days. An additional bed biomass activity test (BBAT) assessing strictly the conversion capacity of the biomass retained in the bed region of the reactors was carried out between days 172 and 182.

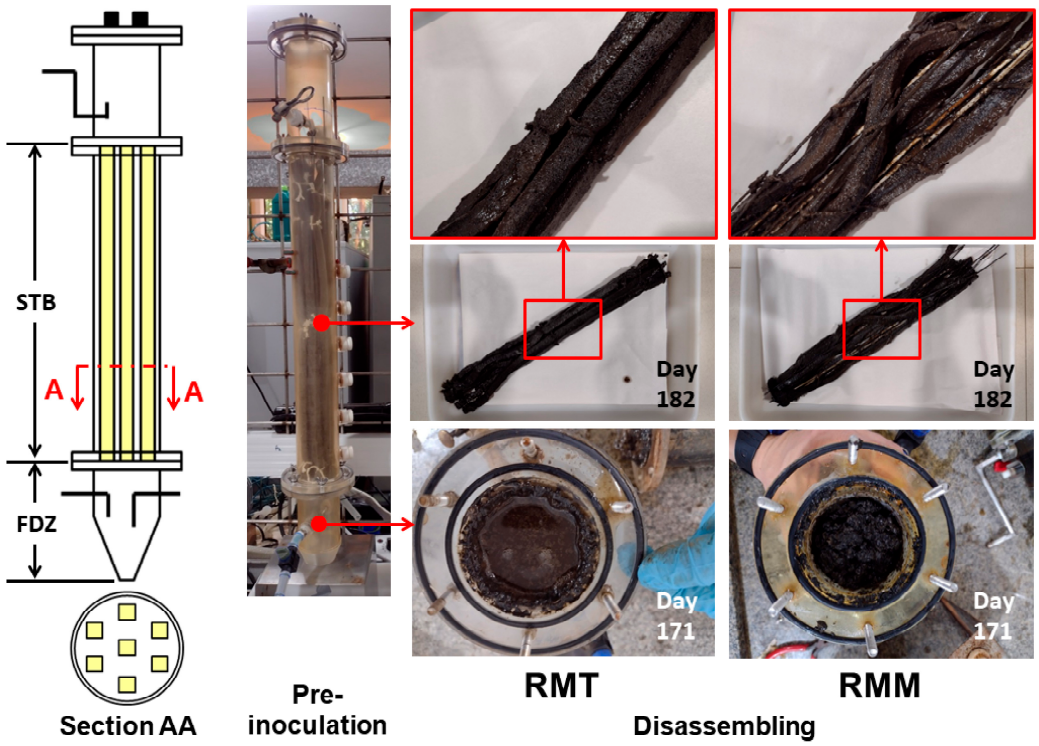

Figure 1. Details of the PU-filled AnSTBR (sketch + assembled reactor) and characteristics of the suspended and attached biomass in the feeding zone (FDZ) and structured bed (STB) of the reactors at the end of the operation. Nomenclature: RMT—thermophilic methanogenic reactor, RMM—mesophilic methanogenic reactor.

Differently from conventional investigations on the AD of sugarcane vinasse, the operation of the reactors simulated sequential periods of season and off-season, using vinasse and molasses (both fermented) as the substrates, respectively. Overall details of the reactors' performance were previously presented elsewhere [18], considering the usual approach based on the temporal monitoring of the reactor operation and the spatial characterization of substrate conversion. Table 1 summarizes the different operating phases assessed and selected performance results (substrate conversion and methane production) relevant to the current study. In addition, Table 2 shows the temporal compositional variability of the fermented substrates, considering the major organic compounds present.

Table 1. Operating conditions applied in the methanogenic reactors and selected performance results—according to Fuess et al. [18].

Substrate		**Fermented Vinasse**		**Fermented Molasses**	**Fermented Vinasse**			**Fermented Vinasse**
Period (d)		1–36	37–68	69–107	108–125	126–153	154–171	172–182
Phase		S1-I	S1-II	OS	S2-I	S2-II	S2-III	BBAT [4]
OLR [1] (kg COD m^{-3} d^{-1})		1.0–7.5	10.0	10.0	10.0	12.5–17.5	20.0	10.0
ER_{COD} [2] (%)	RMT	68.2	77.4	89.5	83.1	77.5	74.5	75.4
	RMM	78.4	80.9	90.6	85.1	81.6	80.3	80.4
$ER_{COD,FDZ}$ [3] (%)	RMT	-	80.7	90.1	82.2	-	75.8	-
	RMM	-	83.7	93.2	83.9	-	77.9	-
ER_{PheOH} (%)	RMT	34.5	38.5	29.5	48.6	43.4	38.1	-
	RMM	50.7	43.0	40.2	58.3	52.8	48.2	-
VOA (mg acetic acid L^{-1})	RMT	-	291	115	50	-	579	-
	RMM	-	175	154	42	-	229	-
MY (NmL CH_4 g^{-1}COD)	RMT	304	330	340	341	334	329	329
	RMM	328	337	342	343	339	334	339

Nomenclature: OLR—organic loading rate; ER_{COD}—removal efficiency of chemical oxygen demand (reactor); $ER_{COD,FDZ}$—removal efficiency of chemical oxygen demand in the feeding zone; ER_{PheOH}—removal efficiency of total phenols; VOA—volatile organic acids; MY—methane yield; RMT—thermophilic methanogenic reactor; RMM—mesophilic methanogenic reactor; S1—season #1; OS—off-season; S2—season #2. [1] Because the HRT was fixed at 24.0 = 1 d, the OLR numerically corresponds to the total chemical oxygen demand (COD, in g L^{-1}). [2] Relative to the total COD (non-centrifuged samples). [3] Relative to the soluble COD (centrifuged samples). [4] Bed biomass activity test carried out to assess the organic matter conversion capacity of the microbial biomass retained in the bed region. Analytical procedures used in the characterization of the substrates are listed in the Supplementary Data Section.

Table 2. Major organic constituents and sulfate availability in the fermented substrates used in reactor feeding.

Operating Period (d)	**1–33**	**34–39**	**50–68**	**69–81**	**82–96**	**97–104**	**105–107**	**108–120**	**121–134**	**135–143**	**144–153**	**154–162**	**163–166**	**167–171**
Substrate	Fermented vinasse			Fermented molasses				Fermented vinasse						
Soluble carbohydrates [1]	4.1	3.5	2.8	17.5	4.2	3.7	5.0	2.6	2.6	3.6	3.1	2.6	2.5	2.2
Lactate [1]	0.3	0.4	0.3	47.2	42.7	50.7	48.1	0.3	0.4	0.4	0.3	0.2	0.2	0.2
Total phenols [1]	12.5	10.1	13.1	2.5	3.1	2.5	2.8	9.1	13.6	12.5	11.2	7.5	10.8	12.7
Ethanol [1]	13.5	11.4	10.6	7.5	11.7	8.8	9.5	12.2	6.9	12.5	8.2	9.2	11.1	zero
Acetate [1]	8.0	9.2	8.4	2.2	3.6	3.4	2.4	7.9	4.9	6.9	10.3	10.8	8.9	14.7
Propionate [1]	2.4	2.4	3.5	0.1	0.7	0.1	0.2	4.1	1.7	1.5	2.5	4.1	3.1	9.6
Butyrate [1]	13.0	14.5	18.9	1.2	10.4	4.7	5.5	20.3	17.9	9.5	16.1	10.9	13.8	6.0
COD/Sulfate [2]	69	57	53	56	107	77	66	201	104	68	26	85	190	94

[1] Values correspond to the percentage (%) relative to the soluble chemical oxygen demand (g COD-compound per g of soluble COD). [2] g COD g^{-1} sulfate. Values are shown in percentages because the COD applied in the reactors varied according to the operating phase (Table 1). Analytical procedures used in the characterization of the substrates are listed in the Supplementary Data Section.

2.2. Quantitative Biomass Characterization

The amount of biomass retained in the reactors after the inoculation step, washed out throughout the entire operating period, and retained in the reactors at the end of the operation was quantified according to different procedures. Given that a blend of diluted vinasse + sludge (known solid content) was recirculated in each reactor during the inoculation [18], the amount of retained biomass before the continuous operation started was calculated from the difference between the total amount of biomass available for recirculation and the amount of biomass remaining in the vessels collecting the recirculated

substrate. The biomass washed out during the continuous operation was determined in effluent samples periodically collected from both reactors. Finally, the amount of biomass retained in the reactors at the end of the continuous operation was collected in two steps.

Once phase S2-III was finalized on day 171 (Table 1), the suspended biomass retained in the feeding zone (FDZ) of the reactors was collected, while the attached biomass retained in the structured bed (STB) was maintained for the complementary BBAT for an additional ten days. Then, the reactors were fully disassembled, and the attached biomass was collected by rinsing the support material (PU) with deionized water. The amount of solids in the bulk liquid of the STB was also quantified. Details of the biomass retained in the different compartments of the reactors are depicted in Figure 1. All solid measurements were carried out in terms of volatile suspended solids (VSS) concentrations, following the protocol described elsewhere [19].

The specific organic loading rate (sOLR), which represents the temporal dynamics of the food-to-microorganism (F/M) ratio in continuous systems, was calculated using the methodology initially described by Anzola-Rojas et al. [20] and further modified elsewhere [21]. Details of the calculations are available in the Supplementary Data Section, including the determination of the biomass growth yield coefficient ($Y_{X/S}$; g VSS g^{-1}COD) and biomass retention rate (BRR).

2.3. Microbial Community Characterization

2.3.1. Biomass Sampling

The microbial community in 12 biomass samples collected from the FDZ and STB of both reactors was characterized using 16S rRNA gene amplicon sequencing. For each reactor the inoculum, four samples collected from the FDZ (in phases S1-II, OS, S2-I, and S2-III; see Table 1 for phase description) and one sample collected from the STB after the bed biomass activity test were analyzed. Focus was given to biomass samples from the FDZ because most of the organic matter conversion (>75%) occurred in this compartment, as shown in spatial characterization profiles carried out throughout the operation of the reactors [18] (details in Table 1). Table 3 shows the nomenclature used in biomass sample identification. After collection, the samples were washed with phosphate-buffered saline in consecutive rounds (2–3) of centrifugation (6000 rpm, 10 min) to remove residual dissolved organic constituents. Biomass pellets were then stored at −20 °C prior to further processing.

Table 3. Details of the biomass samples used in microbial community characterization.

Sample Nomenclature	Phase (OLR [1])	Sampling Details	
		Source/Reactor Compartment	Day [2]
T1, M1	Pre-inoculation (-)	Thermophilic flocculent methanogenic sludge (T), Mesophilic granular methanogenic sludge (M)	-
T2, M2	S1-II (10.0)	FDZ	65
T3, M3	OS (10.0)	FDZ	87
T4, M4	S2-I (10.0)	FDZ	122
T5, M5	S2-III (20.0)	FDZ	171
T6, M6	BBAT (10.0)	STB	182

Nomenclature: OLR—organic loading rate; T—thermophilic methanogenic reactor (RMT); M—mesophilic methanogenic reactor (RMM); FDZ—feeding zone; STB—structured bed; BBAT—bed biomass activity test. [1] kg COD m^{-3} d^{-1}. [2] With reference to day zero of the continuous operation.

2.3.2. DNA Extraction, 16s rRNA Gene Amplicon Sequencing, and Bioinformatics

Genomic DNA extraction using the FastDNA SPIN Kit for soil (MP Biomedicals, Irvine, CA, USA), 16S rRNA gene amplicon sequencing using a MiSeqTM System (Illumina, Inc., San Diego, CA, USA) owned by NGS Soluções Genômicas (Piracicaba, Brazil), and sequence analysis were carried out as described by Fuess et al. [1]. A detailed description of the procedures is presented in the Supplementary Data Section. As a result, a total of

251,603 reads were annotated for the 12 samples (average 25,328 ± 3858), divided into 1547 amplicon sequence variants (ASV) classified to the genus level. The sequences were submitted to the National Center for Biotechnology Information (NCBI) under accession BioProject ID PRJNA1063313.

3. Results and Discussion

3.1. Microbial Biomass Production and Retention

The patterns of biomass production and retention were initially assessed by comparing the amounts of biomass measured after the inoculation step and at the end of the continuous operation. Similar amounts of biomass were quantified in both reactors (FDZ + STB) at the end of the operation, i.e., 46.8 g VSS (RMT) and 43.3 g VSS (RMM). However, the amount of biomass produced and retained in RMT was approximately 50% higher (27.0 g VSS) than in RMM (17.8 g VSS). Because the reactors were operated under equivalent OLR and HRT levels, this result suggests that the cell retention in the thermophilic system was enhanced as a strategy to increase the cell activity (achieving a level like that of the mesophilic reactor) by offsetting the lower amount of biomass retained after the inoculation, i.e., 19.8 g VSS (RMT) vs. 25.7 g VSS (RMM). Regardless of the microbial composition differences (Sections 3.3 and 3.4), the provision of equivalent amounts of substrate (OLR) demands equivalent cell activity to maintain efficient conversion rates, provided that no overloading conditions are achieved.

The terminal biomass distribution, including the suspended, attached, and washed-out fractions, is depicted in Figure 2a,b. Following the similar overall retention pattern, equivalent amounts of biomass were retained in the FDZ, i.e., 13.2 (RMT) vs. 16.6 (RMM) g VSS, and STB, i.e., 31.7 (RMT) vs. 25.5 (RMM) g VSS, of the reactors (Figure 2a,b). Hence, 30–35% of the biomass inserted (through inoculation) and produced in the reactors was maintained within the systems (FDZ + STB; Figure 2a,b). In practical aspects, only the necessary amounts of biomass required to withstand the applied operating conditions in the systems were maintained in the reactors. The observation of equivalent biomass retention in the FDZ is of relevance because it explains the enhanced (and equivalent) conversion of organic matter (>75%, Table 1) observed in this compartment in the spatial characterization profiles presented elsewhere [18].

Interestingly, a very discrepant physical conformation of the microbial biomass was observed in the FDZ of each reactor: while suspended/slightly flocculent cells prevailed in RMT, relatively large granule-like structures (5–10 mm) were observed in RMM (Figure 3a). Given that equivalent feeding conditions were applied in both reactors, i.e., substrate type, feeding flow, and, therefore, upflow velocity, this discrepancy resulted from the different temperature levels or from the inoculum sludge sources (or a combination of both factors). The granular character of the mesophilic sludge (Section 2.1) may have played a determining role in this process. Scanning electron microscopy was used in an exploratory investigation of the "granular" biomass collected from RMM, showing the predominance of coccoid groups mainly at the surface (Figure 3c; most likely *Methanosarcina* archaea; please refer to Section 3.4 for details on the microbial community characterization). The analysis of the material by energy-dispersive X-ray spectroscopy revealed a higher proportion of calcium (8.4%; Figure 3b) in the inner portion of the granule (compared to the surface, 1.6%), a result that corroborates previous results demonstrating that calcium (or more precisely, bivalent cations) plays an important role in biomass aggregation. The dosing of proper amounts of calcium was demonstrated to enhance the formation of different microbial structures, including flocs in activated sludge systems [22], granules in UASB reactors [23,24], and biofilms in fermentative reactors [25]. Research on this topic shows that the interaction between extracellular polymers and bivalent cations forms more stable complexes [23]. Sugarcane vinasse is rich in bivalent cations, including calcium (812–2280 mg L^{-1} [26]; 350–600 mg L^{-1} [27]) and magnesium (164–348 mg L^{-1} [26]; 200–300 mg L^{-1} [27]), which induce granulation when suitable environmental conditions are provided.

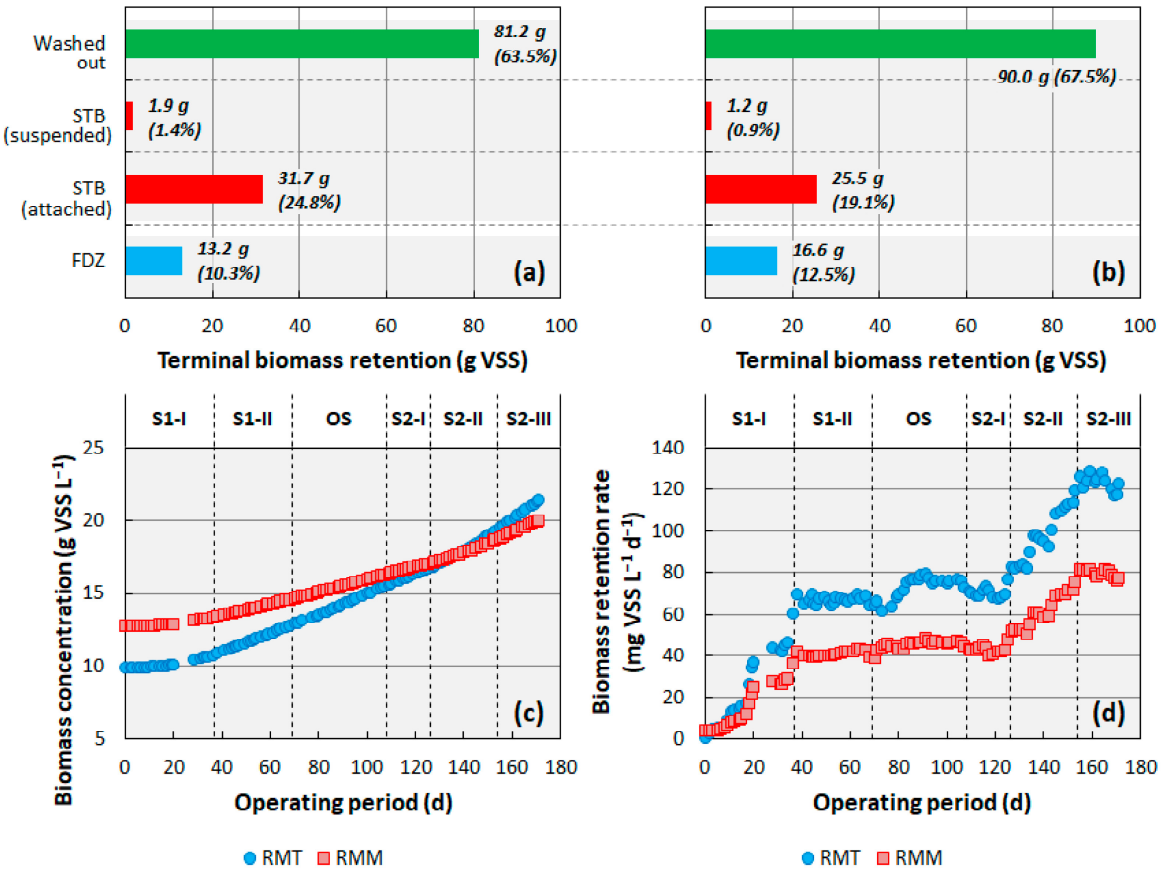

Figure 2. Terminal biomass distribution in the (**a**) RMT and (**b**) RMM; temporal evolution of the (**c**) biomass concentration and (**d**) biomass retention rate in the reactors. Percentage values (parts "a" and "b") refer to the relative distribution of the biomass. Please refer to Table 1 for details on the operating conditions.

The temporal profiles obtained for the biomass concentration (Figure 2c) and BRR (Figure 2d) better represent the dynamics of biomass growth and retention in the reactors, which resulted in the final above-mentioned distribution patterns (Figure 2a,b). A marked increase in biomass concentration was observed only when applying an OLR $\geq$ 5.0 kg COD m^{-3} d^{-1} (from day 19 onwards; Figure 2c), after which discrepant BRR levels were observed in each system (Figure 2d). The biomass concentration in both reactors increased by less than 2% before day 19 (Figure 2c). The application of an OLR < 5.0 kg COD m^{-3} d^{-1} (phase S1-I) characterized a condition of organic underload in the reactors. In practical terms, the relatively low amount of substrate provided did not require a prompt response of the microbial biomass towards enhanced growth. A marked discrepancy in BRR profiles was observed only after applying an OLR of 10 kg COD m^{-3} d^{-1}, with approximately 65% higher values observed in RMT compared to RMM (Figure 2d), i.e., 67 ($\pm$2) vs. 41 ($\pm$1) mg VSS L^{-1} d^{-1} using the mean values observed during phase S1-II as the reference.

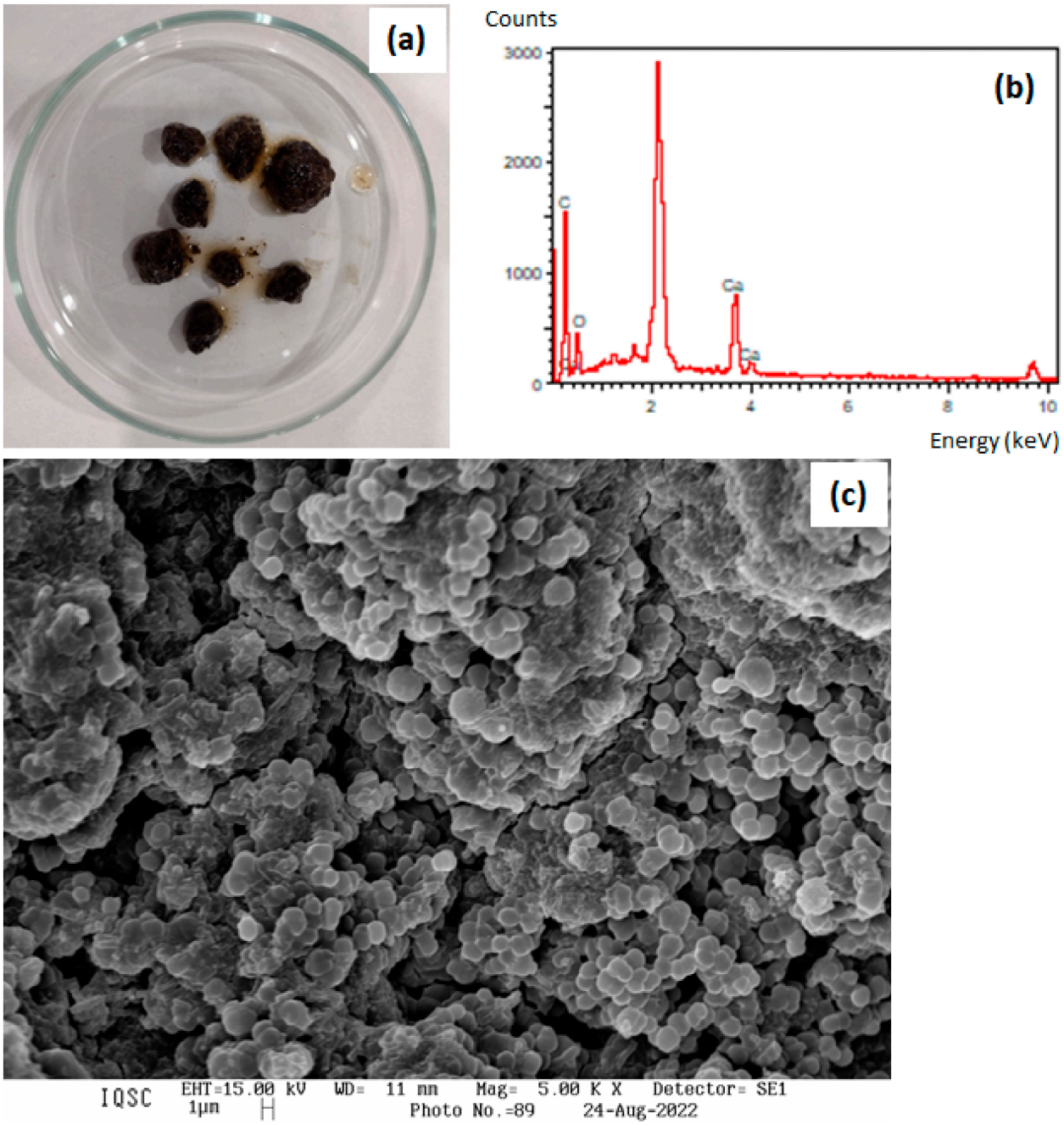

Figure 3. Characterization of the biomass collected from the feeding zone of RMM at the end of the operation: (**a**) granule-like biomass aggregates; (**b**) energy-dispersive X-ray spectroscopy analysis describing the elemental composition in the inner portion of the aggregate (the non-identified peak refers to gold, which was used to metalize the samples); and (**c**) a scanning electron microscopy image of the aggregate's surface.

These results suggest that the microbial biomass in RMM may have reached balanced conditions in terms of retention requirements before RMT, which was most likely favored by the higher amount of biomass preserved in the mesophilic reactor after the inoculation. Approximately 135 d were required for the thermophilic biomass to achieve concentrations equivalent to those of the mesophilic biomass (Figure 2c). The further increase in the OLR (up to 20.0 kg COD m^{-3} d^{-1}) in phases S2-II and S2-III triggered a second period of enhanced BRR (Figure 2d), still characterized by higher values in the case of RMT. It is important to stress that the maintenance of relatively high ER_{COD} (75–80%) and mainly

high MY (329–339 NmL CH_4 g^{-1}COD) values (Table 1) in these conditions indicates the non-occurrence of organic overloads in the reactors, as stated elsewhere [18]. Hence, the thermophilic environment most likely did not trigger enhanced cell decay patterns, providing conditions for maintaining high BRR throughout the entire operating period in RMT. The terminal biomass concentrations predicted by the calculation procedure, i.e., 21.4 g VSS L^{-1} (RMT) and 20.0 g VSS L^{-1} (RMM), reached values slightly underestimated (yet very similar) to those measured, i.e., 23.4 g VSS L^{-1} (RMT) and 21.7 g VSS L^{-1} (RMM).

From a mathematical perspective (see the Supplementary Data Section), the higher biomass retention observed in RMT resulted from a higher fraction of retained biomass (fXr; 0.25 vs. 0.16) compared to RMM. In other words, approximately 25% of the biomass produced in RMT remained in the reactor, while approximately 16% of the amount produced in RMM remained in the system. To achieve the balance in biomass concentration, a higher amount of the produced biomass was removed from RMM, i.e., 84% vs. 75% (RMT). The other parameters used in the calculation reached equivalent values in both systems, including the amount of converted substrate (2876 vs. 3025 g COD in RMT and RMM, respectively, considering the total amount converted) and the $Y_{X/S}$ values: 0.038 g VSS g^{-1}COD (RMT) vs. 0.036 g VSS g^{-1}COD (RMM). The latter result is highly relevant because it demonstrates the capability of microbial communities originating from different sources and performing different methane-producing pathways (Sections 3.3 and 3.4) to behave similarly in quantitative terms when subjected to equivalent operating conditions (specifically in terms of substrate quality and availability, without reaching overloads). Hence, differences in temperature will not be the only factor explaining the biomass growth patterns in fixed-film reactors. Obviously, this result is not directly applicable to suspended-growth reactors.

The literature lacks results on the estimation of $Y_{X/S}$ values in methanogenic fixed-film systems, which limits carrying out a vast comparative analysis. Only two reports assessing the AD of vinasse and molasses provide interesting comparative results. Using fermented molasses as the only substrate in the feeding of two thermophilic (55 °C) PU-filled AnSTBR systems, Fuess et al. [21] reported $Y_{X/S}$ values of 0.028 and 0.039 g VSS g^{-1}COD, like those observed in this study. These authors associated the highest $Y_{X/S}$ with the establishment of an unfavorable environment for the microbial biomass (triggered by organic overloads), which stimulated washout events and, therefore, required higher cell production rates. RMT and the two AnSTBR systems operated by Fuess et al. [21] were inoculated with the same inoculum source (flocculent thermophilic sludge; Section 2.1), showing that the same microbial community responds quantitatively differently when subjected to different operating conditions.

$Y_{X/S}$ values were also obtained in fixed-film reactors, namely, one AnSTBR and one anaerobic packed-bed reactor (AnPBR), both filled with PU, processing fresh vinasse at mesophilic conditions (30 °C) [3]. In this case, the authors observed a marked discrepancy in the $Y_{X/S}$ values, i.e., 0.095 (AnSTBR) vs. 0.067 (AnPBR) g VSS g^{-1}COD, due to the differences in the surface area available for biomass attachment (approximately 6-fold higher in the AnPBR). The higher the surface area, the higher the amount of retained biomass, which decreases the amount of metabolic energy dedicated to growth (lower $Y_{X/S}$) [3,25]. In addition, the low bed porosity of AnPBR systems tends to minimize cell washout, which maintains high cell densities within the reactors and leads to lower $Y_{X/S}$ values. Both factors explain the higher $Y_{X/S}$ in the AnSTBR, despite the utilization of the same source of sludge in the inoculation. The same source of sludge used by Aquino et al. [3] was used in the inoculation of RMM (mesophilic granular sludge; Section 2.1). The different operating conditions (bed conformation, OLR, and HRT) also explain the very discrepant $Y_{X/S}$ observed in these studies.

The type (compositional quality) of the substrate may also have triggered some marked differences in the growth pattern of the mesophilic sludge. Using non-fermented vinasse favors the activity of fermentative bacteria growing on carbohydrates and glycerol (35–40% of the soluble COD) [1], which may explain the higher $Y_{X/S}$ (0.095 g VSS g^{-1}COD) reported by Aquino et al. [3] compared to that observed in RMM (0.036 g VSS g^{-1}COD), both

considering AnSTBR systems. The pre-fermentation of the substrate is expected to favor the occurrence of slow-growing microbes (acetogens and methanogens) in the second-stage methanogenic reactor, resulting in relatively low $Y_{X/S}$ values.

3.2. Specific Organic Loading Rates

The specific organic loading rate, or "dynamic F/M ratio," was assessed relative to the total amount of biomass retained (sOLR, Figure 4a) and to the biomass retained exclusively in the FDZ ($sOLR_{FDZ}$, Figure 4b) and in the STB ($sOLR_{STB}$, Figure 4c) of the reactors. The conditions of organic underload (Section 3.1) were associated with sOLR values (relative to the total amount of biomass) lower than 0.3 g COD g VSS d^{-1} (Figure 4a). Interestingly, the technical literature recommends biological loads (synonym to sOLR) of no more than 0.3–0.4 g COD g vs. d^{-1} (VS = volatile solids) [28] to ensure stability in methanogenic systems (assuming values applied in the case of domestic sewage), potentially characterizing an underestimation of the conversion capability of methanogenic communities. Once the OLR was increased to 10.0 kg COD m^{-3} d^{-1} or more (from day 37 onwards), the sOLR (still relative to the total amount of biomass retained) varied approximately within 0.6–1.0 g COD g VSS d^{-1} (Figure 4a), i.e., approximately 2-fold higher than the recommended levels. Aquino et al. [3] calculated sOLR values ranging between 0.15–0.49 g COD g VSS d^{-1} and 0.05–0.30 g COD g VSS d^{-1} in mesophilic AnSTBR and AnPBR systems fed with fresh sugarcane vinasse. Barros et al. [29] calculated the organic load in the sludge (a parameter equivalent to the sOLR) in mesophilic (20–30 °C) sequential vinasse-fed UASB reactors (both methanogenic), with values in the range of 0.16–0.42 g COD g vs. d^{-1} (first reactor) and 0.15–0.67 g COD g vs. d^{-1} (second reactor). The only report on the measurement of the sOLR in thermophilic methanogenic reactors (AnSTBR systems fed with fermented molasses) [21] indicated values usually lower than 1.0 g COD g VSS d^{-1} in long-term operating periods (230–250 d), peaking at approximately 3.5 g COD g VSS d^{-1}.

The lower amount of biomass retained in RMT after the inoculation step resulted in higher sOLR in this system, mainly when applying OLR levels of 5.0–10.0 kg COD m^{-3} d^{-1} (Figure 4a). Once equivalent retention levels were established in both reactors (approximately day 135), the systems behaved similarly in terms of the sOLR. It is important to stress that the substrate availability at the beginning of phase S1-II (OLR = 10.0 kg COD m^{-3} d^{-1}, sOLR = 1.0–0.9 g COD g^{-1}VSS d^{-1}) was like that in phase S2-III (Figure 4a) in RMT, when the highest OLR was applied in the reactors (20.0 kg COD m^{-3} d^{-1}). These results suggest that the thermophilic reactor was operated under equivalent conditions (despite the differences in the applied OLR) and explain the equivalent performance in phases S1-II (ER_{COD} = 77.4%, MY = 330 NmL CH_4 g^{-1}COD) and S2-III (ER_{COD} = 74.5%, MY = 329 NmL CH_4 g^{-1}COD) (Table 1). Nevertheless, the heterogeneous biomass distribution in the FDZ and STB (Section 3.1) somehow weakens the sOLR calculated in terms of the total amount of retained biomass because the substrate provided to each "microbial community", i.e., the suspended (FDZ) and the attached (STB) biomass, was highly different on both quantitative and qualitative bases. The first group was fed with fermented substrates rich in readily available carbon (organic acids, ethanol, and carbohydrates, Table 2), while the second group was subjected only to the unconverted organic fraction, i.e., organic carbon availability 75–80% (eventually 90% when using molasses) lower than in the FDZ. Hence, assessing the sOLR separately in the FDZ ($sOLR_{FDZ}$) and STB ($sOLR_{STB}$) is a more realistic approach to understanding the processing capability of the methanogenic communities.

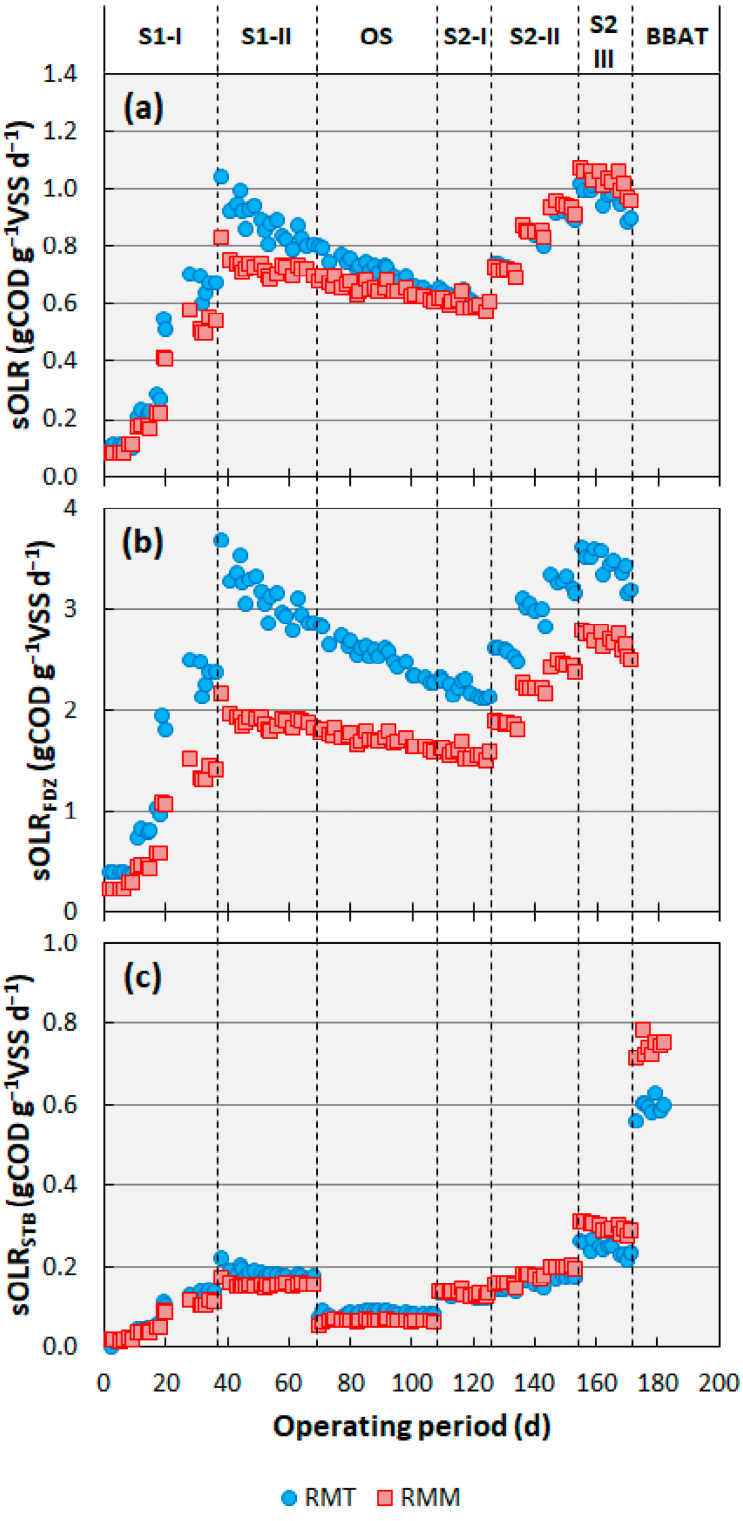

Figure 4. Temporal evolution of the specific organic loading rate relative to (**a**) the total amount of biomass retained in the reactors (sOLR), (**b**) the amount of biomass retained in the feeding zone ($sOLR_{FDZ}$), and (**c**) the amount of biomass retained in the structured bed ($sOLR_{STB}$, including the bed biomass activity test—BBAT—period). Please refer to Table 1 for details on the operating conditions.

The temporal variation in the $sOLR_{FDZ}$ (Figure 4b) revealed a marked discrepancy in both systems: using results obtained from phase S1-II onwards (OLR $\geq$ 10.0 kg COD m^{-3} d^{-1}) as the reference, the $sOLR_{FDZ}$ varied within the ranges of 2.0–3.7 (RMT) and 1.5–2.8 (RMM) g

COD g VSS d^{-1}. In particular, the $sOLR_{FDZ}$ in phases S1-II, OS, and S2-I (OLR = 10.0 kg COD m^{-3} d^{-1}) was always much higher in RMT (values exceeding those in RMM by 35–83%), so that the initial difference in the amount of biomass retained post-inoculation explains this pattern. In practical aspects, the thermophilic biomass was always subjected to a harsher environment in terms of high substrate availability compared to the mesophilic one. Interestingly, the high $sOLR_{FDZ}$ values observed in the reactors were not impeditive to reaching efficient methane production levels, characterized by a MY always higher than 329 NmL CH_4 g^{-1}COD (at least 94% of the theoretical value, i.e., 350 NmL CH_4 g^{-1}COD) for OLR $\geq$ 10.0 kg COD m^{-3} d^{-1} (Table 1). Yet, these $sOLR_{FDZ}$ values are approximately 10-fold higher than the values recommended for the biological load reported elsewhere (0.3–0.4 g COD g vs. d^{-1}) [28].

Assessing the sOLR is of particular interest for identifying the effective occurrence of organic overloads in methanogenic reactors because this parameter describes the real substrate availability. The $sOLR_{FDZ}$ values calculated herein are like the ones observed in a previous experiment on the thermophilic biomethanation of fermented molasses using AnSTBR systems [21]. In this case, the authors also reported the occurrence of stable methane production under $sOLR_{FDZ}$ as high as 3.0 g COD g^{-1}VSS d^{-1}. Additional analyses combining data collected from the aforementioned continuous systems [21] and batch reactors (also producing methane from fermented molasses) [30] indicated that efficient methanogenesis (measured as the methane production rate) would still be observed at sOLR values as high as 5.0 g COD g^{-1}VSS d^{-1}. The combined assessment of these results (including the ones reported in this study) strongly indicates that the degrading capability of methanogenic consortia is frequently underestimated, as evidenced by the F/M ratio, i.e., 0.3–0.5 g COD g^{-1}VSS (or VS) used in batch reactors (e.g., biomethane production tests) [30–32]. These conservative values most likely derive from previous experiences with specific methanogenic activity tests, in which the best results were frequently associated with F/M < 0.5 g COD g^{-1}VSS [33]. In practical terms, the results suggest that methanogenic sludge can withstand sOLR (or biological load) values frequently recommended for fermentative systems (>>1.0 g COD g^{-1}VSS d^{-1}) [20,25], which can be translated into the application of high OLR (provided that microbial consortia are acclimatized to both the substrate and environmental conditions).

The compartmentalized assessment of the sOLR also enabled the investigation of the effective substrate availability in the STB of the reactors ($sOLR_{STB}$, Figure 4c), including the BBAT, in which only the attached biomass was maintained in the systems. Given the high $ER_{COD,FDZ}$ observed in both reactors, regardless of the OLR (Table 1), no more than 15% of the influent COD was applied in the STB. Consequently, $sOLR_{STB}$ values were always below 0.3 g COD g^{-1}VSS d^{-1} (Figure 4c) during the continuous operation. The marked drop in $sOLR_{STB}$ values in phase OS (from approximately 0.2 to approximately 0.1 g COD g^{-1}VSS d^{-1}; Figure 4c) resulted from the higher biodegradable character of fermented molasses compared to fermented vinasse, resulting in higher $ER_{COD,FDZ}$ values in this period (>90%; Table 1). Overall, approximately 70% of the soluble COD in fermented molasses corresponded to organic acids, ethanol, and carbohydrates, while the same compounds accounted for 30–45% of fermented vinasse (Table 2). The relatively lower biodegradable character of vinasse is evidenced by the higher proportions of total phenols (PheOH) compared to molasses (usually > 10% vs. < 3%; Table 2). Overall, the removal efficiency of PheOH (ER_{PheOH}) never exceeded 60% throughout the entire operating period (Table 1). These factors (with the low $sOLR_{STB}$ values characterizing conditions of organic underload) explain the apparent inactivity of the attached biomass during the continuous operation, as reported elsewhere [18].

The $sOLR_{STB}$ markedly increased only during the BBAT, reaching approximately 0.6 and 0.7–0.8 g COD g^{-1}VSS d^{-1} in RMT and RMM, respectively (Figure 4c), i.e., values equivalent to those observed in the FDZ during the application of low OLR (<5.0 kg COD m^{-3} d^{-1}) (Figure 4b). These $sOLR_{STB}$ values indicate an excess amount of biomass compared to the amount of available substrate. Hence, the attached biomass was not

subjected to organic overloads, which explains the maintenance of relatively high ER_{COD} and MY values (Table 1). The compartmentalized assessment of the sOLR suggests that both reactors could withstand higher OLR (>20.0 kg COD m^{-3} d^{-1}) because unconverted biodegradable organic compounds leaving the FDZ (due to an eventual localized organic overload) would most likely be complementarily converted by the attached biomass. Finally, it is important to stress that the patterns describing the biomass distribution and the sOLR described herein do not describe the patterns in larger-scale reactors. The FDZ tends to be proportionally much lower than the bed region in the latter systems, requiring more effective participation of the attached biomass in COD conversion.

3.3. Microbial Community Characterization in RMT

The characterization of the microbial communities in biomass samples collected from RMT (T1–T6; Table 3) at the phylum-class and genus levels is depicted in Figure 5a,b, while a heat map including relevant genera is also provided in the Supplementary Data Section. At the phylum-class level, T1 (inoculum) was composed mainly of *Firmicutes* (25.23%), with *Clostridia* as the most representative class (16.62%), unknown *Hydrothermae* (13.15%), *Thermotogota–Thermotogae* (11.05%), and *Coprothermobacterota–Coprothermobacteria* (10.74%), followed by *Bacteroidota–Bacteroidia* (6.80%) and *Synergistota–Synergistia* (4.13%). Methanogenic archaea belonging to *Methanobacteria* and *Methanosarcinia* accounted for 0.68% and 3.26%, respectively. Other minor classes, i.e., showing relative abundance (RA) < 1%, accounted for 11%. The classes *Incertae Sedis_2*, *Limnochordia* (*Firmicutes*), and *Cloacimonadia* (RA < 1% in T1; Figure 5a) were selected in RMT, with RA varying between 2.92–10.83%, 3.95–12%, and 4–23.44%, respectively. Except for *Coprothermobacteria* and unknown *Hydrothermae*, whose RA dropped to 0.13–5.12% and 0.13–1.99%, respectively, the other phyla-classes were maintained in the reactor with RA values varying according to the operating phases (Figure 5a).

At the genus level (Figure 5b), unknown *Hydrothermae* ASV_7 was the most representative group in T1 (13.15%), followed by *Coprothermobacter* ASV_27 (6.43%), *Defluviitoga* ASV_38 (6.13%), *Lentimicrobium* ASV_6 (3.75%), *Acetomicrobium* ASV_40 (2.63%), *Incertae Sedis_2*-DTU014 ASV_5 (1.84%), and D8A-2 ASV_49 (1.21%) in minor abundance. The hydrogenotrophic methanogenic *Methanothermobacter* [34] and the metabolically versatile *Methanosarcina* [35] were detected with RA of 0.68% and 2.52%, respectively. Other minor genera (RA < 1%) comprised 57.91% of the ASV and included members of the *Clostridia* class. In this class, *Caldicoprobacter* ASV_37 was the only genus whose RA increased during the operation, reaching 2.35% (T5) and 2.40% (T6) (Figure 5b). The aforementioned genera with RA > 1% were not selected in RMT, with the exception of *Incertae Sedis_2*-DTU014 and *Lentimicrobium*. All genera found in T1 have been associated with thermophilic fermentation of carbohydrates and proteins, syntrophic VOA oxidation, aromatic compound degradation, and biogas production [36–38].

The primary microbial groups with low RA in T1 and selected in RMT were *Mesotoga* ASV_1 (3.09–23.31%) and *Cloacimonadaceae*-W5 ASV_3 (4–23.44%), followed by *Hydrogenispora* ASV_12 (0.96–7.78%), *Limnochordia*-MBA03 ASV_18 (0.47–4.53%) and ASV_31 (0.26–2.52%), and unknown *Kapabacteriales* ASV_36 (0.32–2.07%), unknown *Pelotomaculum* ASV_44 (0.60–2.10%), and *Anaerolinea* ASV_45 (0.20–1.65%) in minor frequency (Figure 5b). *Methanotermobacter* was also selected (0.36–3.46%), while the RA of *Methanosarcina* tended to decrease (0.52–1.93%), showing that hydrogenotrophic methanogenesis prevailed in the reactor (Figure 5b). Microbial groups of both the Bacteria and Archaea domains evolved differently according to the operating conditions applied in RMT (Figure 5b; please also refer to the Supplementary Data Section).

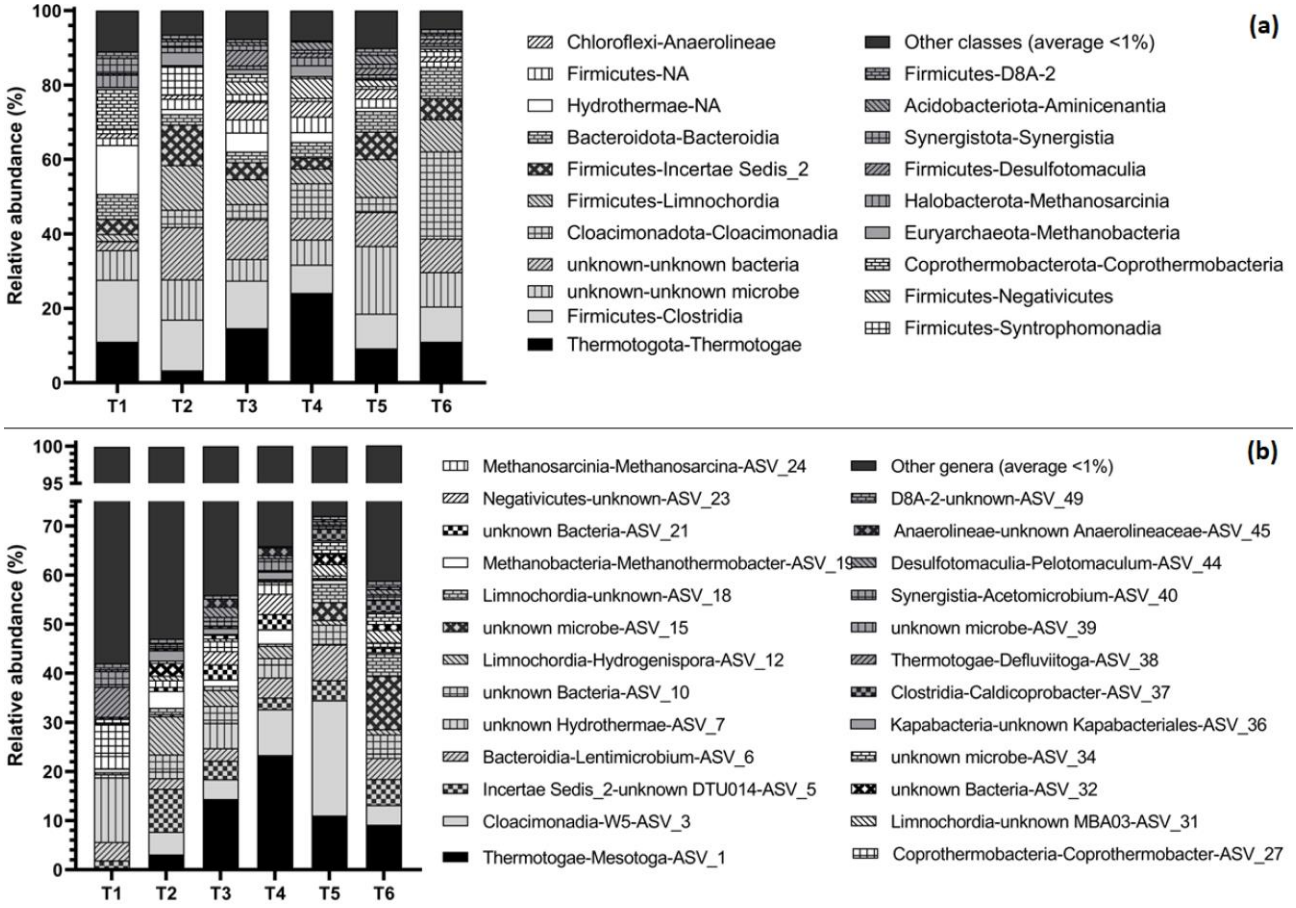

Figure 5. Taxonomic distribution according to the 16S rRNA gene amplicon sequencing at the (**a**) phylum-class level and (**b**) genus level of the biomass samples collected from the thermophilic inoculum (T1) and from RMT (T2–T6). Please refer to Table 3 for details on the biomass sample description.

At the end of operating phase S1-II, *Incertae Sedis*_2-DTU014 and *Hydrogenispora* were dominant with RA of 8.71% and 7.78%, respectively, followed by *Cloacimonadaceae*-W5 (4.65%), *Mesotoga* (3.09%), *Lentimicrobium* (2.15%), *Limnochordia*-MBA03 (2.13% considering all ASV), and unknown *Kapabacteriales* (2.07%) (sample T2; Figure 5b). Although not shown in Figure 5b, the known syntrophic butyrate oxidizers *Syntrophothermus* ASV_52 and *Syntrophomonas* ASV_67 were also detected with RA of 2.07% and 2.52%, respectively. *Hydrogenispora* and *Lentimicrobium* ferment glucose to produce acetate, hydrogen, and propionate [39,40] and were most likely involved in the fermentation of residual carbohydrates found in fermented vinasse. The metagenomic assembled genome (MAG) of *Kapabacteriales* suggests acetate utilization, although the mechanism remains unclear [41]. *Incertae Sedis*_2-DTU014, *Limnochordia*-MBA03, and *Mesotoga* have been associated with syntrophic acetate oxidation, while *Syntrophothermus* and *Syntrophomonas* with syntrophic butyrate oxidation and *Cloacimonadaceae*-W5 with syntrophic propionate oxidation, all pathways directly or indirectly supplying hydrogenotrophic methanogens with H_2 and CO_2 [30,42–46]. The butyrate-rich fermented vinasse (Table 2) initially selected syntrophic oxidizers whose association with methanogenic archaea efficiently converted COD into methane, with $ER_{COD,FDZ}$ of 80.7%, low effluent VOA concentrations, and MY of 330 NmL CH_4 g^{-1}COD (Table 1). Even though it is unclear whether *Methanosarcina* (1.39%; sample T2) performed acetoclastic or hydrogenotrophic methanogenesis, the selection of strictly hydrogenotrophic *Methanothermobacter* (RA of 3.46%; Figure 5b) in addition to the high RA of syntrophic acetate-oxidizing bacteria (RA of 14% considering all ASV) strongly suggests that hydrogenotrophic methanogenesis was the main methane-producing pathway in RMT,

as also observed by Vilela et al. [47] and Fuess et al. [30] in thermophilic reactors fed with fermented molasses.

The replacement of vinasse by molasses in phase OS triggered important shifts in the microbial community of RMT (sample T3; Table 3) by selecting mainly *Mesotoga* (14.40%), followed by unknown *Hydrothermae* (5.12%), unknown *Negativutes* (2.68%), *Pelotomaculum* (2.10%), and *Anaerolinea* (1.65%) (Figure 5b). Meanwhile, the RA of unknown *Hydrogenispora* (3.25%), *Incertae Sedis_2*-DTU014 (3.79%), *Limnochordia*-MBA03 (1.32%), and *Syntrophothermus* (1.25%) decreased relative to phase S1-II (sample T2; Figure 5b). *Cloacimonadaceae*-W5 and *Lentimicrobium* ASV_6 were not affected by the molasses feeding, preserving similar RA, i.e., 4.02% and 2.52%, respectively. Carbohydrate-rich (17.5% of the soluble COD) fermented molasses was initially used as the substrate in phase OS (days 69–81; Table 2), which was further replaced by carbohydrate-poor samples (<5.0%; Table 2) from day 82 onwards. Lactate always prevailed as the main organic compound in fermented molasses (42.7–50.7%; Table 2). The biomass sample was collected in a transition between the periods of high and low carbohydrate availability at day 87 (Table 3).

The high initial carbohydrate content in molasses favored fermentation, mediated most likely by *Mesotoga*, unknown *Hydrothermae*, *Anaerolinea*, unknown *Hydrogenispora*, *Lentimicrobium,* and unknown *Negativicutes*. *Negativicutes* cover members known to produce acetate, propionate, butyrate, and valerate, in addition to CO_2 and low amounts of H_2 from lactic acid and glucose fermentation [48,49]. *Mesotoga* could also be involved in syntrophic carbohydrate oxidation coupled with hydrogenotrophic methanogenesis [50]. The high proportion of lactate in molasses (Table 2) most likely favored the growth of unknown *Negativicutes* and *Pelotomaculum*, which syntrophically oxidize lactate, producing acetate and H_2 coupled with hydrogenotrophic methanogenesis [51].

The dominance of *Mesotoga* in fermented molasses shows that, somehow, this genus was selected at high lactate availability. *Mesotoga infera* is able to oxidize lactate to acetate and H_2 in the presence of elemental sulfur [52]. Although elemental sulfur was not detected in fermented molasses and is not expected to occur in an oxygen-free environment like the RMT, the known capability of *Mesotoga* to oxidize carbohydrates and VOA [50,52] suggests that lactate oxidation was driven by an unknown mineral or was coupled with hydrogenotrophic methanogenesis. In addition, *Mesotoga* and *Syntrophothermus* most likely oxidized the relatively high butyrate concentrations also present in fermented molasses. The minor propionate concentrations were syntrophically oxidized by *Cloacimonadaceae*-W5 and *Pelotomaculum*, while syntrophic acetate oxidation was most likely mediated by *Incertae Sedis_2*-DTU014, *Limnochordia*-MBA03, and *Mesotoga*. Although phase OS selected bacteria related to acetate production and consumption via syntrophic oxidation coupled with hydrogenotrophic methanogenesis, the RA of *Methanothermobacter* and *Methanosarcina* decreased to 1.27% and 0.88%, respectively, when compared with sample T2 (Figure 5b). It is important to stress that a malfunctioning of the peristaltic pump used for RMT feeding between days 70 and 74 negatively impacted the methanogenic activity during phase OS [18]. Because the biomass sampling was carried out on day 87 (Table 3), the length of the operating period may have been relatively short to detect any increase in the genome abundance of these archaeal genera after the disturbance. Nevertheless, they were highly active, as demonstrated by the high $ER_{COD,FDZ}$ (90.1%), low residual VOA concentration (115 mg acetic acid L^{-1}), and high MY (340 NmL CH_4 g^{-1}COD) (Table 1).

The re-introduction of fermented vinasse in phase S2-I further triggered an additional marked shift in the microbial community of RMT (sample T4; Figure 5b). The RA of the genera *Mesotoga*, *Cloacimonadacea*-W5, *Lentimicrobium,* and unknown *Negativicutes* peaked at 23.31%, 9.34%, 4.09%, and 4.15%, respectively, while unknown *Hydrothermae* dropped to 2.67% (Figure 5b). The abundances of *Incertae Sedis_2*-DTU014, *Limnochordia*-MBA03, and unknown *Hydrogenispora*, characterized by decreases during phase OS (sample T3), did not recover with the re-introduction of fermented vinasse, reaching values of 2.38%, 0.47%, and 2.67%, respectively. *Methanothermobacter* and *Methanosarcina* were re-established, reaching RA of 2.86% and 1.93%, respectively, values similar to phase S1-II. The selection of

Mesotoga showed that this microbial group outcompeted other syntrophic acetate oxidizers, such as *Incertae Sedis_2*-DTU014 and *Limnochordia*-MBA03. The predominance of *Mesotoga*, *Cloacimonadacea*-W5, *Lentimicrobium,* and unknown *Negativicutes,* in addition to the re-establishment of methanogenic archaea, shows that fermented molasses selected anaerobes whose growth was also favored in fermented vinasse, efficiently coupling syntrophic VOA oxidation with hydrogenotrophic methanogenesis. The higher substrate conversion ($ER_{COD,FDZ}$ of 82.2%), much lower residual VOA concentration (50 mg acetic acid L^{-1}), and higher MY (342 NmL CH_4 g^{-1}COD) (Table 1) compared to phase S1-II corroborate this finding.

Mesotoga was negatively affected by the increase in the OLR (20.0 kg COD m^{-3} d^{-1}) in phase S2-III (Table 1), with the RA decreasing to 11.04% (Figure 5b). Unknown *Hydrothermae* and *Hydrogenispora* failed to grow under these conditions, while the RA of *Incertae Sedis_2*-DTU014 increased to 4.10%, and the RA of *Cloacimonas*-W5, *Lentimicrobium,* and *Limnochordia*-MBA03 peaked at 23.44%, 7.28%, and 6.07%, respectively. *Caldicoprobacter*, a group previously related to syntrophic acetate oxidation [45], reached an RA of 2.35%. Apart from the increase in the OLR, lower butyrate proportions were observed in fermented vinasse when compared to the substrate utilized in previous phases, while the proportion of both propionate and acetate consistently increased (Table 2). The relatively low proportion of butyrate impaired the growth of *Mesotoga*, even with the high proportion of acetate, while the higher availability of propionate stimulated the growth of the syntrophic propionate oxidizer *Cloacimonas*-W5. The limited growth of *Mesotoga* most likely favored the growth of other acetate-oxidizing groups, such as *Incertae Sedis_2*-DTU014 and *Limnochordia*-MBA03. However, excess acetate was neither efficiently metabolized by the syntrophic association between acetate oxidizers and hydrogenotrophic methanogens nor directly consumed by *Methasarcina*. The RA of *Methanosarcina* and *Methanothermobacter* dropped, respectively, to 0.75% and 0.52%, which was accompanied by the build-up of VOA (559 mg acetic acid L^{-1}) and drops in both the $ER_{COD,FDZ}$ (75.8%), and MY (329 NmL CH_4 g^{-1}COD) (Table 1).

The microbial community in the STB (sample T6) was similar to that observed in the FDZ in phase S2-III (sample T5). *Mesotoga*, *Limnochordia*-MBA03, *Incertae Sedis_2*-DTU014, *Lentimicrobium,* and *Cloacimonas*-W5 were the main genera, with RA of 9.16%, 7.05%, 5.31%, 4.29%, and 4%, respectively (Figure 5b). *Caldicoprobacter* (2.40%) and unknown *Hydrogenispora* (1.06%) were found in minor abundances (Figure 5b). The RA of *Mesotoga* and *Cloacimonas*-W5 decreased when compared to T5, as well as the methanogenic archaea *Methanothermobacter* (0.36%) and *Methanosarcina* (0.78%) (Figure 5b). The use of propionate- and acetate-rich fermented vinasse in the BBAT negatively affected the syntrophic propionate oxidizer *Cloacimonas*-W5 and the syntrophic acetate oxidizer *Mesotoga*, with no apparent effect on *Limnochordia*-MBA03 and *Incertae Sedis_2*-DTU014. Once again, excess acetate was neither efficiently metabolized by syntrophic acetate oxidizers coupled to hydrogenotrophic methanogens nor consumed by *Methanosarcina*, resulting in a relatively low $ER_{COD,FDZ}$ (75.4%) and MY (329 NmL CH_4 g^{-1}COD), similar to those observed in phase S2-III (Table 1).

In addition to high VOA proportions, ethanol accounted for a relatively high fraction of the soluble COD (usually 10–12%; Table 2) of both vinasse and molasses. Interestingly, *Pelotomaculum* was the only known syntrophic ethanol oxidizer [51] detected in RMT at RA >1% (only in samples T3 and T6; Figure 5b). This genus has been related to thermophilic phenol and phthalate degradation in association with hydrogenotrophic methanogens [53], characterizing the only known bacteria related to this metabolism detected in RMT. These results strongly suggest that ethanol and mainly phenol degradation were restricted to *Pelotomaculum* in RMT. Nevertheless, some unknown groups could also have mediated ethanol and phenol conversion in the reactor: unknown bacteria ASV10, ASV21, ASV32, and unknown microbes ASV39 were present in all operating phases, with RA varying within the ranges of 1.32–3.90%, 0.18–3.12%, 0.73–2.62%, and 0.41–1.83%, respectively. In addition, the proportion of unknown microbes ASV15 increased in sample T5 (3.61%)

and peaked at sample T6 (10.83%) (Figure 5b), showing that the use of propionate- and acetate-rich fermented vinasse favorably selected this group, mainly in the STB.

3.4. Microbial Community Characterization in RMM

Figure 6 shows details of the microbial community at the phylum-class and genus levels in biomass samples collected from RMM, including the inoculum. Relevant genera are complementarily presented in the Supplementary Data Section. At the phylum-class level, the mesophilic inoculum (sample M1) showed a diverse composition, with *Gammaproteobacteria* (15%), *Bacteroidota–Bacteroidia* (12%), *Cloacimonadota–Cloacomonadia* (11%), *Desulfobacterota–Syntrophia* (8%) and *Campilobacterota–Campylobacteria* (7%) identified as the most abundant groups, followed by *Firmicutes–Clostridia* (4%), *Chloroflexi–Anaerolineae* (4%) and *Verrucomicrobiota–Verrucomicrobiae* (2%) at lower frequency (Figure 6a). Classes with RA < 1%, unknown microbes, and unknown bacteria accounted for 20%, 14%, and 2%, respectively. Regarding methanogenic archaea, *Methanosarcinia* was the only class detected (RA of 0.6%).

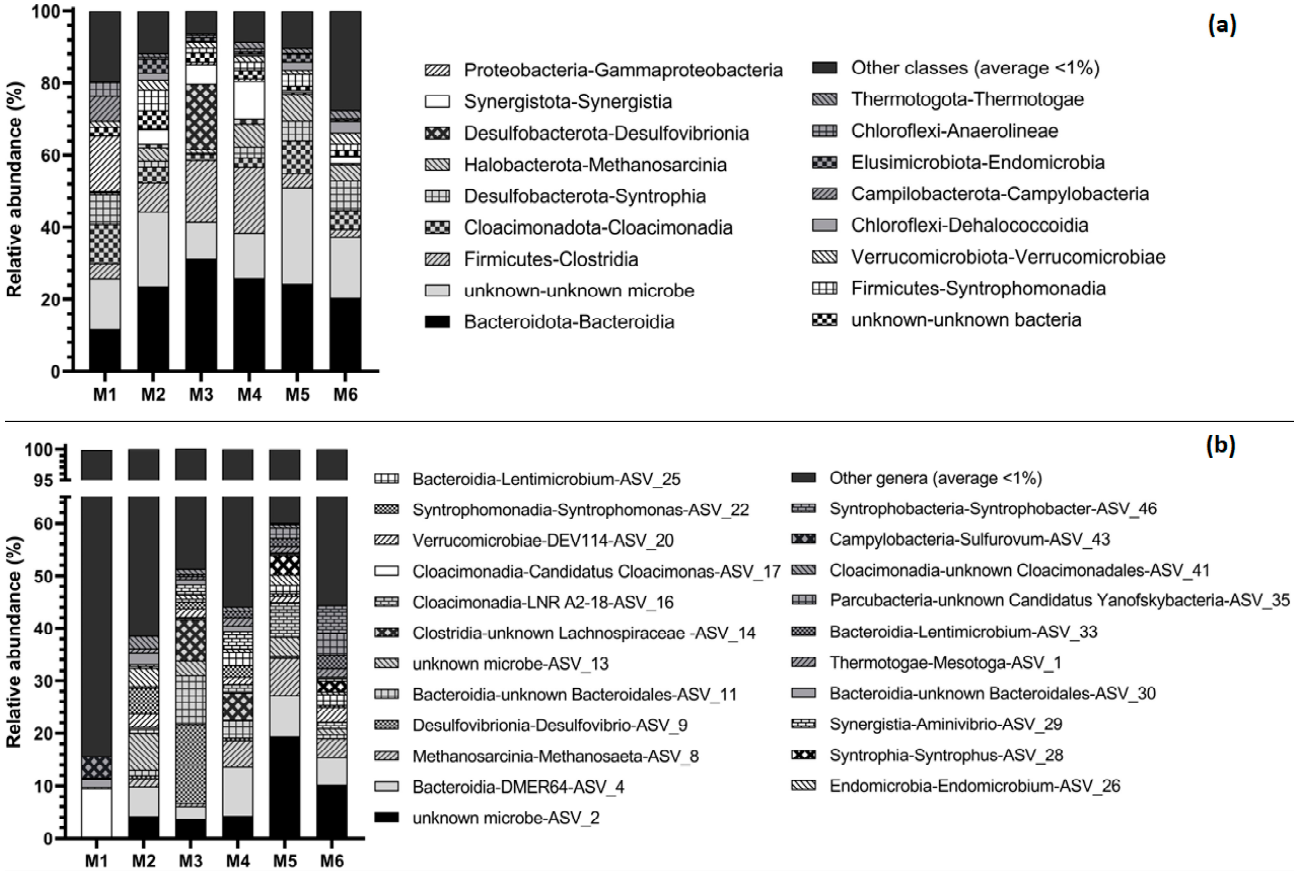

Figure 6. Taxonomic distribution according to the 16S rRNA gene amplicon sequencing at the (**a**) phylum-class level and (**b**) genus level of the biomass samples collected from the mesophilic inoculum (M1) and from RMM (M2–M6). Please refer to Table 3 for details on the biomass sample description.

These results are similar to those reported by Delforno et al. [54] while studying the same type of inoculum. These authors also reported the presence of functional genes related to fermentation, syntrophic oxidation of VOA, anaerobic degradation of aromatic compounds, and methanogenesis. The microbial composition and abundance of the classes that grew favorably in RMM differed from sample M1 without showing defined patterns in the sequential operating phases. *Gammaproteobacteria* and *Campylobacteria* failed to grow, while the RA of *Syntrophia* decreased in the FDZ (0.3–5.6%) and remained relatively high in

the STB (8%) (Figure 6a). The RA of *Cloacomonadia* varied between 1.6 and 9%, reaching the peak at sample M5, and *Anaerolineae* decreased from 4% to 0.2–1% in both the FDZ and STB (Figure 6a). Meanwhile, *Bacteroidia* (20–31%) and *Clostridia* (2–18%) were selected during the operating phases, as well as some groups with RA < 1% in sample M1, such as *Synergistota–Synergistia* (0.5–10%), *Desulfobacterota–Desulfovibrionia* (0.4–18%), *Thermotogota–Thermotogae* (0.1–2%), and *Methanosarcinia* (1–7%). *Elusimicrobiota–Endomicrobia* (0.5–4%), *Chloroflexi–Dehalococcoidia* (0.3–3%), and *Firmicutes–Syntrophomonadia* (1.4–5.6%), although virtually not detected in sample M1, were also selected in RMM. The shift in microbial classes relative to the inoculum most likely resulted from both the type of substrate (poultry slaughterhouse wastewater vs. fermented vinasse and molasses) and the gradual increase in the OLR (Figure 6a). In addition, the replacement of vinasse by molasses during the operating phase OS selected *Bacteroidia* (31%), *Clostridia* (17%), and *Desulfovibrionia* (18%) in sample M3 (Figure 6a).

Most ASV in sample M1 (82%) were detected at very low RA (<1%; Figure 6b) at the genus level, while a few ASV were more abundant (RA > 1%), such as *Candidatus Cloacimonas* ASV_17 (9.5%), *Sulfurovum* ASV_43 (4.06%), and unknown *Bacteroidales* ASV_30 (1.45%). *Sulfurovum* covers chemolithoautotrophic sulfur-oxidizing bacteria [55], which failed to grow in RMM, most likely due to the very low availability of sulfur in the fermented substrates (Table 2). Meanwhile, *C. Cloacimonas* remained at a lower RA compared to sample M1, and *Bacteroidales* was selected in the reactor (RA of 8.57% considering all ASV). *C. Cloacimonas* is an acetogen with metabolic potential for syntrophically oxidizing propionate [56,57], while members of *Bacteroidales* are involved in the degradation of carbohydrates, amino acids, and phenol [58–60].

Similarly to the phylum-class level, rare genera (RA < 1%) and those virtually not detected in sample M1 were favored during the operation of RMM. *Syntrophorhabdus*, a genus detected in sample M1 (1.20%; Figure 6b), degrades phenol in association with hydrogenotrophic methanogens [61,62]. The presence of this group explains the high phenol removal efficiency observed during the inoculation of RMM (70.6%) [18]. However, *Syntrophorhabdus* failed to grow in the reactor, a pattern that derived from the prevalence of acetoclastic methanogenesis in RMM, with the selection of *Methanosaeta* ASV_8 (Figure 6b). Nevertheless, the genus *Syntrophus* ASV_28 was selected in RMM (0.18–3.63%; Figure 6b), covering members capable of degrading benzoate, a key intermediate of phenol degradation, while producing acetate by fermentative metabolism [63,64] or acetate and H_2 in co-culture with H_2- and acetate-utilizing microorganisms [65,66]. Hence, the selection of *Syntrophus* indirectly indicates the occurrence of phenol degradation in RMM, explaining the moderate-to-high phenol removal efficiency (40.2–58.3%; Table 1) observed during the operation. Moreover, the phylum *Bacteroidota* was also selected in RMM (Figure 6a), which has also been related to phenol degradation in anaerobic reactors fed with vinasse [60].

Bacteroidia-DMER64 ASV_4 (5.69%), *Syntrophomonas* ASV_22 (4.81%), *Endomicrobium* ASV_26 (3.52%), *Verrucomicrobia*-DEV114 ASV_20 (2.73%), unknown *Cloacimonadales* ASV_41 (2.30%), unknown *Bacteroidales* ASV_30 (2.19%), and ASV_11 (1.12%) were the dominant genera in phase S1-II (sample M2; Figure 6b). *Methanosaeta* ASV_8 was the only methanogenic archaea detected (1.52%) (Figure 6b), and all remaining genera showed an RA < 1% (Figure 6b). The potential to syntrophically oxidize propionate and butyrate has been attributed to *Bacteroidia*-DMER64, a group capable of mediating direct interspecies electron transfer (DIET) in association with several methanogenic archaea, including *Methanosaeta* [67,68]. *Syntrophomonas* also covers propionate and butyrate oxidizers, which may also mediate DIET using pilli structures [69]. The butyrate-rich fermented vinasse (Table 2) potentially favored the growth of these groups in direct association with *Methanosaeta* in RMM, explaining the enhanced substrate uptake ($ER_{COD,FDZ}$ of 83.7%; Table 1) and methane production (MY of 337 NmL CH_4 g^{-1}COD; Table 1). VOA utilized in this syntrophic association may have also been produced *in loco* by *Endomicrobium*, *Bacteroidales*, and *Cloacimonadota* through the fermentation [56,59,70,71] of residual carbohydrates present in vinasse.

The replacement of fermented vinasse by fermented molasses in phase OS also triggered marked shifts in the microbial community established in RMM, with the selection of *Desulfovibrio* ASV_9 (15.05%), unknown *Bacteroidales* ASV_11 (9.34%), and unknown *Lachnospiraceae* ASV_14 (7.84%) (sample M3; Figure 6b). A RA < 2% was observed for the other genera, including *Methanosaeta* (0.57%) (Figure 6b). In the absence of sulfate, *D. vulgaris* grows syntrophically on lactate with H_2-consuming partners, such as *Methanococcus maripaludis* [72]. The oxidation of lactate has also been associated with *Bacteroidales* with a high degree of genetic redundancy with *D. vulgaris* [73]. *Lachnospiraceae* is metabolically versatile, covering members involved in carbohydrate fermentation, autotrophic, and mixotrophic acetogenesis [74–86]. Lactate accounted for approximately 50% of the soluble COD in fermented molasses (Table 2) and was efficiently degraded in RMM (99.9%) [18]. The microbial community selected strongly suggests lactate was oxidized into acetate, CO_2, and H_2 by *Desulfovribio* and unknown *Bacteroidales*, with the further consumption of H_2/CO_2 by unknown *Lachnospiraceae* to produce acetate (homoacetogenesis), which was further converted to methane by *Methanosaeta*. Kim et al. [77] and Detman et al. [73] reported the prevalence of acetoclastic methanogenesis in the presence of lactate because lactate degradation requires the lowest energy input and provides the highest energy gain for acetate-producing bacteria when compared with the oxidation of butyrate and propionate. In addition, the participation of hydrogenotrophic methanogens is not required. It is important to stress that the RA of *Methanosaeta* decreased in sample M3 when compared to sample M2 (Figure 6b). However, this trend was not an impediment to the maintenance of a high methanogenic activity, characterized by a MY of 342 NmL CH_4 g^{-1}COD and an $ER_{COD,FDZ}$ of 93.2% (Table 1).

The re-introduction of fermented vinasse in phase S2-I (sample M4) further shifted the microbial community composition in RMM (Figure 6b). *Desulfovibrio* ASV_9, unknown *Bacteirodales* ASV_11, and unknown *Lachnospiraceae* ASV_14 were negatively affected by shifting the substrate, as evidenced by marked decreases in RA values from 15.05% to 0.48% (ASV_9), from 9.34% to 3.24% (ASV_11), and from 7.84% to 5.14% (ASV_14) (Figure 6b). This result shows that *Desulfovibrio* was restricted to lactate oxidation, while unknown *Bacteirodales* and *Lachnospiraceae*, although affected by the low lactate availability (Table 2), were able to metabolize the other organic sources and intermediates abundantly available in vinasse. *Bacteroidia*-DMER64 and *Methanosaeta* were re-established in the reactor, reaching a RA of 9.37% and 5.02%, respectively, values higher than those observed in phase S1-II (sample M2; Figure 6b). *Syntrophomonas* was also re-established (2.19%), while the growth of *Aminivibrio* ASV_29 (3.23%), *Lentimicrobium* ASV_25 (2.58%), *Mesotoga* ASV_1 (1.60%) and *Cloacimonadia*-LNR A2–18 ASV_16 (1.56%), was favored once RA < 1% was observed for all these genera at the beginning of the operation in phase S1-II (sample M2; Figure 6b).

TBC 1, the only *Lentimicrobium* species, ferments glucose to produce acetate, malate, propionate, formate, and H_2 [40]. *Mesotoga* covers members that ferment sugars and proteins, with acetate as the major end product [78], as well as members that oxidize carbohydrates coupled with hydrogenotrophic methanogens and sulfate-reducing bacteria [50]. In addition, syntrophic acetate oxidation has also been attributed to *Mesotoga* coupled with hydrogenotrophic methanogens [44], as discussed in Section 3.3. *A. pyruvatiphilus*, the only species of *Aminivibrio*, ferments amino acids and organic acids, producing acetate, propionate, H_2, and CO_2 [79], and *Cloacimonadata* genomes encode genes involved in acidogenesis and acetogenesis, including propionate oxidation [56]. The microbial community established in phase S2-I (sample M4) was metabolically more efficient than that established in phase S1-II (sample M2), considering the enhanced growth of acetate producers directly supplying *Methanosaeta*. The higher $ER_{COD,FDZ}$ (83.9%), and MY (343 NmL CH_4 g^{-1}COD), as well as the lower VOA concentration (42 mg acetic acid L^{-1}) (Table 1), support this finding.

Increasing the OLR to 20.0 kg COD m^{-3} d^{-1} in phase S2-III (sample M5) impaired the growth of *Bacteroidia*-DMER64 (RA of 7.92%) but favored *Methanosaeta* (7.02%), *Cloacimonadia*-LNR A2-18 (6.69%), *Syntrophus* (3.63%), and *Lentimicrobium* ASV_35 (1.96%) (Figure 6b).

Endomicrobium was re-established (1.98%), while the RA of *Syntrophomas*, *Aminivibrio*, *Lentimicrobium* ASV_25, and *Mesotoga* slightly decreased (Figure 6b). The dominance of *Bacteroidia*-DMER 64 and *Methanosaeta* clearly shows that these groups were favored by the composition of fermented vinasse, as also observed in samples M2 and M4, and were not affected by the increase in the OLR. Vinasse samples utilized in phase S2-III were richer in acetate (10–15%) and propionate (3–10%) than the vinasse used in previous phases (Table 2). The high propionate availability most likely favored the growth of *Cloacimonadia*-LNR A2-18 over *Bacteroidia*-DMER 64, which oxidizes propionate and butyrate. The increase in the RA of *Methanosaeta* derived from the high concentrations of acetate promptly available in fermented vinasse and produced *in loco* by *Cloacimonadia*-LNR A2-18, *Bacteroidia*-DMER 64, *Syntrophus,* and *Lentimicrobium* through the oxidation of VOA, describing an efficient syntrophic association despite the high OLR. The maintenance of high substrate conversion ($ER_{COD,FDZ}$ of 77.9%), high MY (334 NmL CH_4 g^{-1}COD), and relatively low VOA concentration compared to RMT (229 vs. 579 mg acetic acid L^{-1}) (Table 1) support this finding.

The presence of *Parcubacteria*-unknown *Candidatus Yanofskybacteria* ASV_35 (1.96%) in sample M5 (Figure 6b) deserves special attention because Kuroda et al. [80] showed parasitism between Ca. *Yanofskybacteria* and *Methanothrix* in a methanogenic reactor. Ca. *Yanofskybacteria* lacks most of the genes for biosynthetic pathways, living attached to the *Methanothrix*, deforming its filaments, and causing a loss of activity. Although the RA of *Methanosaeta* reached 7.02% in sample M5, the value dropped to 3.64% in sample M6 (Figure 6b), while the RA of Ca. *Yanofskybacteria* peaked at 4.14%, suggesting parasitism between these microbes. Although the RA of some genera decreased in sample M6 when compared to sample M5, such as *Bacteroidia*-DMER 64 (5.21%), *Cloacimonadia*-LNR A2-18 (1.22%), *Syntrophus* (1.96%), and *Endomicrobium* (0.47%) (Figure 6b), other genera with similar metabolic functions were enriched in the bed region, such as *Syntrophobacter* ASV_46 (5.35%), *Lentimicrobium* (RA of 4.64% considering all ASV), *Verrucomicrobia*-DEV 114 (2.75%), and *Mesotoga* (1.67%). Overall, the microbial community established in the STB followed patterns like those observed in the FDZ, with a strong association between VOA-oxidizing bacteria and *Methanosaeta*, in addition to some fermenters and phenol-degrading individuals. This explains the maintenance of high $ER_{COD,FDZ}$ (80.4%), and MY (339 NmL CH_4 g^{-1}COD) (Table 1), regardless of the complete removal of the biomass from the FDZ during the BBAT.

With respect to ethanol degradation, only one group (*Desulfovibrio*), notably known for oxidizing this compound into acetate, was clearly identified in RMM, showing an RA > 1% only in sample M3 (relative to phase OS when molasses was used as the substrate) (Figure 6b). The low abundance of ethanol oxidizers was a common trend in both reactors, reinforcing the hypothesis that unknown microorganisms actively participated in ethanol conversion. Among the unknown groups, ASV_2 (3.79–19.4%, with the peak observed in sample M5) and ASV_13 (2.78–6.89%, with the peak observed in sample M2) most likely played a relevant role in substrate conversion in RMM.

3.5. Overall Result Interpretation

The results show that, among different factors deeply exploited in the literature, e.g., diversified operating conditions [3,4,18], success in the AD of sugarcane vinasse is achievable because efficient substrate conversion can be mediated by microbial communities with very different composition profiles. In other words, "changing the order of the factors", namely, the prevalence of acetoclastic (mesophilic) or hydrogenotrophic (thermophilic) methanogenesis, "does not affect the product" (methane). Provided that the operating conditions are stable, each microbial consortium will find a balance point (in quantitative terms) at which efficient substrate conversion towards methane-rich biogas is maintained. It is worth noting that limitations in the availability of mesophilic or thermophilic inocula should not be used as an excuse for not implementing full-scale sugarcane vinasse AD plants. Considering the inocula used in this study, both were obtained from full-scale

AD systems, indicating the eventual availability of large amounts of seed sludge. Despite the speculative burden, it is also plausible considering that using other sources of inoculum, such as manure [81], would produce positive results in vinasse AD, mainly under mesophilic conditions.

It is also important to highlight some aspects of the methodological approach adopted in this study. First, understanding the behavior of anaerobic systems by quantifying biomass distribution and using specific parameters, in which the term "specific" means "divided by or relative to the amount of biomass," provides the clearest basis to compare different systems once the effective amount of substrate available for microbial conversion is defined. For instance, the operation of reactors subjected to equivalent OLR levels may not be effectively equivalent if marked differences in biomass retention levels are observed, which will produce different sOLR values. Nevertheless, working with frequent determinations of volatile solid concentrations is laborious, so the implementation of such an approach in the monitoring routine of full-scale systems is highly challenging. Determining the sOLR in running reactors is another equally challenging point [82].

Second, considering the characterization of the microbial communities, it is important to be aware of the possible limitations of the chosen analysis once the presence of a gene does not indicate whether the enzyme is active or not. It is highly recommended to carry out studies based on RNA activity determination, such as in the case reported by Borges et al. [83], as well as other molecular tools that enable determining microbial groups that are not only present in the sample but are also actively carrying out their metabolic functions. Nonetheless, the long-term characterization of the microbial communities in both reactors showed a clear picture of the prevailing aptitudes of each methanogenic consortium, which is useful for defining strategies to operate the whole two-stage AD system. A good example refers to determining the minimum acetate concentrations to be obtained in the fermentative reactor based on the primary acetate consumers in the methanogenic reactor, i.e., acetoclastic methanogens or syntrophic acetate oxidizers.

Additional references describing the methods used in substrate (vinasse and molasses) characterization [84–89] and the molecular analyses [90–98] are found in the Supplementary Data Section.

4. Conclusions

This study demonstrated that temperature (specifically within the mesophilic and thermophilic ranges) impacts the microbial composition but not the overall biomass growth patterns in the biodigestion of sugarcane vinasse in fixed-film reactors subjected to equivalent organic loading rates (OLR). From a quantitative perspective, the community grows and reaches a balance (between retention and washout) defined by the amount of substrate available for conversion. To treat OLR of up to 20.0 kg COD m^{-3} d^{-1}, approximately 30–35% of the microbial biomass produced from vinasse/molasses degradation (approximately 45 g VSS) needed to be retained in the reactors, regardless of the temperature. This similar amount of biomass was concomitant to the association between very different microbial groups, now showing a strong dependence on temperature. While hydrogenotrophic methanogens (mainly *Methanothermobacter*) coupled to syntrophic acetate-oxidizers prevailed at thermophilic conditions, the *Methanosaeta*-mediated acetoclastic pathway occurred in the mesophilic reactor. In both cases, success strongly depended on the syntrophic oxidation of organic acids and ethanol to directly (*Methanosaeta*) or indirectly (*Methanothermobacter*) supply methanogens. In practical aspects, these results show that sugarcane vinasse offers conditions for the establishment of highly efficient anaerobic consortia regardless of the operating conditions, and selecting a processing temperature depends on secondary aspects, such as the preferences in heat management applied in the biorefinery and the availability of inoculum sources.

Supplementary Materials: The following supporting information can be downloaded at: https://www.mdpi.com/article/10.3390/pr12071356/s1, S1. Analytical methods used in reactor monitoring; Table S1: Analytical methods used in the monitoring of the methanogenic reactors (liquid, gas, and solid phases included) [19,84–89]; S2. Specific organic loading rate calculation [20,21]; S3. DNA extraction, 16S rRNA gene amplicon sequencing, and bioinformatics [1,90–98]; Figure S1: Heat map analysis of the most abundant genera in biomass samples collected from the thermophilic inoculum (T1) and from RMT (T2–T6); Figure S2: Heat map analysis of the most abundant genera in biomass samples collected from the mesophilic inoculum (M1) and from RMM (M2–M6).

Author Contributions: Conceptualization, L.T.F. and M.N.d.A.; methodology, L.T.F., F.T.S. and G.B.G.; validation, L.T.F.; formal analysis, L.T.F.; investigation, L.T.F., F.T.S. and G.B.G.; writing—original draft preparation, L.T.F. and F.T.S.; writing—review and editing, L.T.F., M.N.d.A., F.T.S., G.B.G., M.Z. and P.N.L.L.; visualization, L.T.F.; supervision, M.Z. and P.N.L.L.; funding acquisition, M.Z. and P.N.L.L. All authors have read and agreed to the published version of the manuscript.

Funding: This research was funded by SCIENCE FOUNDATION IRELAND (SFI) through the SFI Research Professorship Programme entitled *Innovative Energy Technologies for Biofuels, Bioenergy, and a Sustainable Irish Bioeconomy* (IETSBIO^3; grant number 15/RP/2763) and the Research Infrastructure Research Grant *Platform for Biofuel Analysis* (Grant Number 16/RI/3401); and by SÃO PAULO RESEARCH FOUNDATION (FAPESP; Grant Number 2015/06246-7).

Data Availability Statement: Data will be made available by the authors upon reasonable request.

Acknowledgments: The authors thank Borja Khatabi Soliman Tamayo and Marlee Wasserman (NUIG, Ireland), as well as Carolina A.S. Mirandola, Eloisa Pozzi, Maria A.T. Adorno, and Ana Claudia de Godoy Curro (USP, Brazil), for their help and support during the laboratory work.

Conflicts of Interest: The authors declare no conflicts of interest. The funders had no role in the design of the study, in the collection, analysis, or interpretation of data, in the writing of the manuscript, or in the decision to publish the results.

References

1. Fuess, L.T.; Braga, A.F.M.; Eng, F.; Gregoracci, G.B.; Saia, F.T.; Zaiat, M.; Lens, P.N.L. Solving the bottlenecks of sugarcane vinasse biodigestion: Impacts of temperature and substrate exchange on sulfate removal during dark fermentation. *Chem. Eng. J.* **2023**, *455*, 140965. [CrossRef]
2. Craveiro, A.M.; Soares, H.M.; Schmidell, W. Technical aspects and cost estimations for anaerobic systems treating vinasse and brewery/soft drink wastewaters. *Water Sci. Technol.* **1986**, *18*, 123–134. [CrossRef]
3. Aquino, S.; Fuess, L.T.; Pires, E.C. Media arrangement impacts cell growth in anaerobic fixed-bed reactors treating sugarcane vinasse: Structured vs. randomic biomass immobilization. *Bioresour. Technol.* **2017**, *235*, 219–228. [CrossRef] [PubMed]
4. Del Nery, V.; Alves, I.; Damianovic, M.H.R.Z.; Pires, E.C. Hydraulic and organic rates applied to pilot scale UASB reactor for sugar cane vinasse degradation and biogas generation. *Biomass Bioenergy* **2018**, *119*, 411–417. [CrossRef]
5. Souza, M.E.; Fuzaro, G.; Polegato, A.R. Thermophilic anaerobic digestion of vinasse in pilot plant UASB reactor. *Water Sci. Technol.* **1992**, *25*, 213–222. [CrossRef]
6. Fuess, L.T.; Kiyuna, L.S.M.; Ferraz Júnior, A.D.N.; Persinoti, G.F.; Squina, F.M.; Garcia, M.L.; Zaiat, M. Thermophilic two-phase anaerobic digestion using innovative fixed-bed reactor for enhanced organic matter removal and bioenergy recovery from sugarcane vinasse. *Appl. Energy* **2017**, *189*, 480–491. [CrossRef]
7. van Lier, J.B.; Hulsbeek, J.; Stams, A.J.M.; Lettinga, G. Temperature susceptibility of thermophilic methanogenic sludge: Implications for reactor start-up and operation. *Bioresour. Technol.* **1993**, *43*, 227–235. [CrossRef]
8. Ferraz Júnior, A.D.N.; Etchebehere, C.; Zaiat, M. High organic loading rate on thermophilic hydrogen production and metagenomic study at an anaerobic packed-bed reactor treating a residual liquid stream of a Brazilian biorefinery. *Bioresour. Technol.* **2015**, *186*, 81–88. [CrossRef]
9. Fuess, L.T.; Zaiat, M.; Nascimento, C.A.O. Novel insights on the versatility of biohydrogen production from sugarcane vinasse via thermophilic dark fermentation: Impacts of pH-driven operating strategies on acidogenesis metabolite profiles. *Bioresour. Technol.* **2019**, *286*, 121379. [CrossRef]
10. Niz, M.Y.K.; Etchelet, I.; Fuentes, L.; Etchebehere, C.; Zaiat, M. Extreme thermophilic condition: An alternative for long-term biohydrogen production from sugarcane vinasse. *Int. J. Hydrogen Energy* **2019**, *44*, 22876–22887. [CrossRef]
11. Amani, T.; Nosrati, M.; Mousavi, S.M.; Elyasi, S. Study of microbiological and operational parameters in thermophilic syntrophic degradation of volatile fatty acids in an upflow anaerobic sludge blanket reactor. *J. Environ. Chem. Eng.* **2015**, *3*, 507–514. [CrossRef]
12. Noor, R. Mechanism to control the cell lysis and the cell survival strategy in stationary phase under heat stress. *SpringerPlus* **2015**, *4*, 599. [CrossRef] [PubMed]

13. Infantes, D.; González del Campo, A.; Villaseñor, J.; Fernández, F.J. Influence of pH, temperature and volatile fatty acids on hydrogen production by acidogenic fermentation. *Int. J. Hydrogen Energy* **2011**, *36*, 15595–15601. [CrossRef]
14. Shaw, G.T.W.; Liu, A.C.; Weng, C.Y.; Chou, C.Y.; Wang, D. Inferring microbial interactions in thermophilic and mesophilic anaerobic digestion of hog waste. *PLoS ONE* **2017**, *12*, e0181395. [CrossRef] [PubMed]
15. Maleki, F.; Khosravi, A.; Nasser, A.; Taghinejad, H.; Azizian, M. Bacterial Heat Shock Protein Activity. *J. Clin. Diagn. Res.* **2016**, *10*, BE01–BE03. [CrossRef] [PubMed]
16. Roncarati, D.; Scarlato, V. Regulation of heat-shock genes in bacteria: From signal sensing to gene expression output. *FEMS Microbiol. Rev.* **2017**, *41*, 549–574. [CrossRef] [PubMed]
17. Venkiteshwaran, K.; Bocher, B.; Maki, J.; Zitomer, D. Relating Anaerobic Digestion Microbial Community and Process Function: Supplementary Issue: Water Microbiology. *Microbiol. Insights* **2015**, *8s2*, 37–44. [CrossRef] [PubMed]
18. Fuess, L.T.; Braga, A.F.M.; Zaiat, M.; Lens, P.N.L. Solving the seasonality issue in sugarcane biorefineries: High-rate year-round methane production from fermented sulfate-free vinasse and molasses. *Chem. Eng. J.* **2023**, *478*, 147432. [CrossRef]
19. APHA; AWWA; WEF. *Standard Methods for the Examination of Water and Wastewater*, 22nd ed.; APHA: Washington, DC, USA, 2012.
20. Anzola-Rojas, M.P.; Fonseca, S.G.; Silva, C.C.; Oliveira, V.M.; Zaiat, M. The use of the carbon/nitrogen ratio and specific organic loading rate as tools for improving biohydrogen production in fixed-bed reactors. *Biotechnol. Rep.* **2015**, *5*, 46–54. [CrossRef]
21. Fuess, L.T.; Zaiat, M.; Nascimento, C.A.O. Thermophilic biodigestion of fermented sugarcane molasses in high-rate structured-bed reactors: Alkalinization strategies define the operating limits. *Energy Convers. Manag.* **2021**, *239*, 114203. [CrossRef]
22. Sobeck, D.C.; Higgins, M.J. Examination of three theories for mechanisms of cation-induced bioflocculation. *Water Res.* **2002**, *36*, 527–538. [CrossRef] [PubMed]
23. Yu, H.Q.; Tay, J.H.; Fang, H.H.P. The roles of calcium in sludge granulation during uasb reactor start-up. *Water Res.* **2001**, *35*, 1052–1060. [CrossRef]
24. Batstone, D.J.; Landelli, J.; Saunders, A.; Webb, R.I.; Blackall, L.L.; Keller, J. The influence of calcium on granular sludge in a full-scale UASB treating paper mill wastewater. *Water Sci. Technol.* **2002**, *45*, 187–193. [CrossRef] [PubMed]
25. Blanco, V.M.C.; Fuess, L.T.; Zaiat, M. Calcium dosing for the simultaneous control of biomass retention and the enhancement of fermentative biohydrogen production in an innovative fixed-film bioreactor. *Int. J. Hydrogen Energy* **2017**, *42*, 12181–12196. [CrossRef]
26. Fuess, L.T.; Garcia, M.L.; Zaiat, M. Seasonal characterization of sugarcane vinasse: Assessing environmental impacts from fertirrigation and the bioenergy recovery potential through biodigestion. *Sci. Total Environ.* **2018**, *634*, 29–40. [CrossRef] [PubMed]
27. Piffer, M.A.; Zaiat, M.; Nascimento, C.A.O.; Fuess, L.T. Dynamics of sulfate reduction in the thermophilic dark fermentation of sugarcane vinasse: A biohydrogen-independent approach targeting enhanced bioenergy production. *J. Environ. Chem. Eng.* **2021**, *9*, 105956. [CrossRef]
28. Chernicharo, C.A.L. *Anaerobic Reactors*, 1st ed.; IWA Publishing: London, UK, 2007.
29. Barros, V.G.; Duda, R.M.; Oliveira, R.A. Biomethane production from vinasse in upflow anaerobic sludge blanket reactors inoculated with granular sludge. *Braz. J. Microbiol.* **2016**, *47*, 628–639. [CrossRef] [PubMed]
30. Fuess, L.T.; Eng, F.; Bovio-Winkler, P.; Etchebehere, C.; Zaiat, M.; Nascimento, C.A.O. Methanogenic consortia from thermophilic molasses-fed structured-bed reactors: Microbial characterization and responses to varying food-to-microorganism ratios. *Braz. J. Chem. Eng.* **2022**. [CrossRef]
31. Fuess, L.T.; Piffer, M.A.; Zaiat, M.; Nascimento, C.A.O. Phase separation enhances bioenergy recovery in sugarcane vinasse biodigestion: Absolute or relative truth? *Bioresour. Technol. Rep.* **2022**, *18*, 101026. [CrossRef]
32. Borges, A.V.; Fuess, L.T.; Alves, I.; Takeda, P.Y.; Damianovic, M.H.R.Z. Co-digesting sugarcane vinasse and distilled glycerol to enhance bioenergy generation in biofuel-producing plants. *Energy Convers. Manag.* **2021**, *250*, 114897. [CrossRef]
33. Aquino, S.F.; Chernicharo, C.A.L.; Foresti, E.; Santos, M.L.F.; Monteggia, L.O. Methodologies for determining the specific methanogenic activity (SMA) in anaerobic sludges. *Eng. Sanit. Ambient.* **2007**, *12*, 192–201. [CrossRef]
34. Wasserfallen, A.; Nölling, J.; Pfister, P.; Reeve, J.; Macario, E.C. Phylogenetic analysis of 18 thermophilic *Methanobacterium* isolates supports the proposals to create a new genus, *Methanothermobacter* gen. nov., and to reclassify several isolates in three species, *Methanothermobacter thermautotrophicus* comb. nov., *Methanothermobacter wolfeii* comb. nov., and *Methanothermobacter marburgensis* sp. nov. *Int. J. Syst. Evol. Microbiol.* **2000**, *50*, 43–53. [PubMed]
35. Buan, N.; Kulkarni, G.; Metcalf, W. Genetic methods for *Methanosarcina* species. *Methods Enzymol.* **2011**, *494*, 23–42.
36. Barros, V.G.; Duda, R.M.; Vantini, J.S.; Omori, W.P.; Ferro, M.I.T.; Oliveira, R.A. Improved methane production from sugarcane vinasse with filter cake in thermophilic UASB reactors, with predominance of *Methanothermobacter* and *Methanosarcina* archaea and *Thermotogae* bacteria. *Bioresour. Technol.* **2017**, *244*, 371–381. [CrossRef] [PubMed]
37. Zamorano-López, N.; Greses, S.; Aguado, D.; Seco, A.; Borrás, L. Thermophilic anaerobic conversion of raw microalgae: Microbial community diversity in high solids retention systems. *Algal Res.* **2019**, *41*, 101533. [CrossRef]
38. Camargo, F.P.; Sakamoto, I.K.; Delforno, T.P.; Midoux, C.; Duarte, I.C.S.; Silva, E.L.; Bize, A.; Varesche, M.B.A. Microbial and functional characterization of granulated sludge from full-scale UASB thermophilic reactor applied to sugarcane vinasse treatment. *Environ. Technol.* **2022**, *44*, 3141–3160. [CrossRef] [PubMed]
39. Liu, Y.; Qiao, J.T.; Yuan, X.Z.; Guo, R.B.; Qiu, Y.L. *Hydrogenispora ethanolica* gen. nov., sp. nov., an anaerobic carbohydrate-fermenting bacterium from anaerobic sludge. *Int. J. Syst. Evol. Microbiol.* **2014**, *64*, 1756–1762. [CrossRef] [PubMed]

40. Sun, L.; Toyonaga, M.; Ohashi, A.; Tourlousse, D.M.; Matsuura, N.; Meng, X.Y.; Tamaki, H.; Hanada, S.; Cruz, R.; Yamaguchi, T.; et al. *Lentimicrobium saccharophilum* gen. nov., sp. nov., a strictly anaerobic bacterium representing a new family in the phylum *Bacteroidetes*, and proposal of *Lentimicrobiaceae* fam. nov. *Int. J. Syst. Evol. Microbiol.* **2016**, *66*, 2635–2642. [CrossRef]
41. Al-Saud, S.; Florea, K.M.; Webb, E.A.; Thrash, J.C. Metagenome-Assembled Genome Sequence of *Kapabacteriales* Bacterium Strain Clear-D13, Assembled from a Harmful Algal Bloom Enrichment Culture. *Microbiol. Resour. Announc.* **2020**, *9*, e01118-20. [CrossRef]
42. Nobu, M.K.; Narihiro, T.; Rinke, C.; Kamagata, Y.; Tringe, S.G.; Woyke, T.; Liu, W.T. Microbial dark matter ecogenomics reveals complex synergistic networks in a methanogenic bioreactor. *ISME J.* **2015**, *9*, 1710–1722. [CrossRef]
43. Mosbæk, F.; Kjeldal, H.; Mulat, D.G.; Albertsen, M.; Ward, A.J.; Feilberg, A.; Nielsen, J.L. Identification of syntrophic acetate-oxidizing bacteria in anaerobic digesters by combined protein-based stable isotope probing and metagenomics. *ISME J.* **2016**, *10*, 2405–2418. [CrossRef]
44. Wang, H.Z.; Lv, X.M.; Yi, Y.; Zheng, D.; Gou, M.; Nie, Y.; Hu, B.; Nobu, M.K.; Narihiro, T.; Tang, Y.Q. Using DNA-based stable isotope probing to reveal novel propionate- and acetate-oxidizing bacteria in propionate-fed mesophilic anaerobic chemostats. *Sci. Rep.* **2019**, *9*, 17396. [CrossRef] [PubMed]
45. Dyksma, S.; Jansen, L.; Gallert, C. Syntrophic acetate oxidation replaces acetoclastic methanogenesis during thermophilic digestion of biowaste. *Microbiome* **2020**, *8*, 105. [CrossRef] [PubMed]
46. Xie, Z.; Meng, X.; Ding, H.; Cao, Q.; Chen, Y.; Liu, X.; Li, D. The synergistic effect of rumen cellulolytic bacteria and activated carbon on thermophilic digestion of cornstalk. *Bioresour. Technol.* **2021**, *338*, 125566. [CrossRef] [PubMed]
47. Vilela, R.S.; Fuess, L.T.; Saia, F.T.; Silveira, C.R.M.; Oliveira, C.A.; Andrade, P.A.; Langenhoff, A.; van der Zaan, B.; Cop, F.; Gregoracci, G.B.; et al. Biofuel production from sugarcane molasses in thermophilic anaerobic structured-bed reactors. *Renew. Sustain. Energy Rev.* **2021**, *144*, 110974. [CrossRef]
48. Marounek, M.; Fliegrova, K.; Bartos, S. Metabolism and some characteristics of ruminal strains of *Megasphaera elsdenii*. *Appl. Environ. Microbiol.* **1989**, *55*, 1570–1573. [CrossRef] [PubMed]
49. Louis, P.; Flint, H.J. Formation of propionate and butyrate by the human colonic microflora. *Environ. Microbiol.* **2017**, *19*, 29–41. [CrossRef] [PubMed]
50. Fadhlaoui, K.; Ben Hania, W.; Armougom, F.; Bartoli, M.; Fardeau, M.L.; Erauso, G.; Brasseur, G.; Aubert, C.; Hamdi, M.; Brochier-Armanet, C.; et al. Obligate sugar oxidation in *Mesotoga* spp., phylum *Thermotogae*, in the presence of either elemental sulfur or hydrogenotrophic archaea sulfate-reducers as electron acceptor. *Environ. Microbiol.* **2018**, *20*, 281–292. [CrossRef]
51. Imachi, H.; Sekiguchi, Y.; Kamagata, Y.; Hanada, S.; Ohashi, A.; Harada, H. *Pelotomaculum thermopropionicum* gen. nov., sp. nov., an anaerobic, thermophilic, syntrophic propionate-oxidizing bacterium. *Int. J. Syst. Evol. Microbiol.* **2002**, *52*, 1729–1735.
52. Ben Hania, W.; Postec, A.; Aüllo, T.; Ranchou-Peyruse, A.; Erauso, G.; Brochier-Armanet, C.; Hamdi, M.; Ollivier, B.; Saint-Laurent, S.; Magot, M.; et al. *Mesotoga infera* sp. nov., a mesophilic member of the order *Thermotogales*, isolated from an underground gas storage aquifer. *Int. J. Syst. Evol. Microbiol.* **2013**, *63*, 3003–3008. [CrossRef]
53. Chen, C.L.; Wu, J.H.; Liu, W.T. Identification of important microbial populations in the mesophilic and thermophilic phenol-degrading methanogenic consortia. *Water Res.* **2008**, *42*, 1963–1976. [CrossRef] [PubMed]
54. Delforno, T.P.; Lacerda Júnior, G.V.; Noronha, M.F.; Sakamoto, I.K.; Varesche, M.B.A.; Oliveira, V.M. Microbial diversity of a full-scale UASB reactor applied to poultry slaughterhouse wastewater treatment: Integration of 16S rRNA gene amplicon and shotgun metagenomic sequencing. *MicrobiologyOpen* **2017**, *6*, e00443. [CrossRef] [PubMed]
55. Ju, F.; Zhang, T. Novel Microbial Populations in Ambient and Mesophilic Biogas-Producing and Phenol-Degrading Consortia Unraveled by High-Throughput Sequencing. *Microb. Ecol.* **2014**, *68*, 235–246. [CrossRef] [PubMed]
56. Johnson, L.A.; Hug, L.A. *Cloacimonadota* metabolisms include adaptations in engineered environments that are reflected in the evolutionary history of the phylum. *Environ. Microbiol. Rep.* **2022**, *14*, 520–529. [CrossRef]
57. Westerholm, M.; Calusinska, M.; Dolfing, J. Syntrophic propionate-oxidizing bacteria in methanogenic systems. *FEMS Microbiol. Rev.* **2022**, *46*, fuab057. [CrossRef] [PubMed]
58. Mei, R.; Nobu, M.K.; Narihiro, T.; Liu, W.T. Metagenomic and Metatranscriptomic Analyses Revealed Uncultured *Bacteroidales* Populations as the Dominant Proteolytic Amino Acid Degraders in Anaerobic Digesters. *Front. Microbiol.* **2020**, *11*, 593006. [CrossRef] [PubMed]
59. Iltchenco, J.; Peruzzo, V.; Magrini, F.E.; Marconatto, L.; Torres, A.P.; Beal, L.L.; Paesi, S. Microbiota profile in Mesophilic biodigestion of sugarcane vinasse in batch reactors. *Water Sci. Technol.* **2021**, *84*, 2028–2039. [CrossRef] [PubMed]
60. Menezes, C.A.; Almeida, P.S.; Camargo, F.P.; Delforno, T.P.; Oliveira, V.M.; Sakamoto, I.K.; Varesche, M.B.A.; Silva, E.L. Two problems in one shot: Vinasse and glycerol co-digestion in a thermophilic high-rate reactor to improve process stability even at high sulfate concentrations. *Sci. Total. Environ.* **2023**, *862*, 160823. [CrossRef]
61. Qiu, Y.L.; Hanada, S.; Ohashi, A.; Harada, H.; Kamagata, Y.; Sekiguchi, Y. *Syntrophorhabdus aromaticivorans* gen. nov., sp. nov., the First Cultured Anaerobe Capable of Degrading Phenol to Acetate in Obligate Syntrophic Associations with a Hydrogenotrophic Methanogen. *Appl. Environ. Microbiol.* **2008**, *74*, 2051–2058. [CrossRef]
62. Ju, F.; Wang, Y.; Zhang, T. Bioreactor microbial ecosystems with differentiated methanogenic phenol biodegradation and competitive metabolic pathways unraveled with genome-resolved metagenomics. *Biotechnol. Biofuels* **2018**, *11*, 135. [CrossRef]
63. Schöcke, L.; Schink, B. Energetics and biochemistry of fermentative benzoate degradation by *Syntrophus gentianae*. *Arch. Microbiol.* **1999**, *171*, 331–337. [CrossRef]

64. Elshahed, M.S.; McInerney, M.J. Benzoate Fermentation by the Anaerobic Bacterium *Syntrophus aciditrophicus* in the Absence of Hydrogen-Using Microorganisms. *Appl. Environ. Microbiol.* **2001**, *67*, 5520–5525. [CrossRef] [PubMed]
65. Schöcke, L.; Schink, B. Energetics of methanogenic benzoate degradation by *Syntrophus gentianae* in syntrophic coculture. *Microbiology* **1997**, *143*, 2345–2351. [CrossRef] [PubMed]
66. Jackson, B.E.; Bhupathiraju, V.K.; Tanner, R.S.; Woese, C.R.; McInerney, M.J. *Syntrophus aciditrophicus* sp. nov., a new anaerobic bacterium that degrades fatty acids and benzoate in syntrophic association with hydrogen-using microorganisms. *Arch. Microbiol.* **1999**, *171*, 107–114. [CrossRef]
67. Lee, J.; Koo, T.; Yulisa, A.; Hwang, S. Magnetite as an enhancer in methanogenic degradation of volatile fatty acids under ammonia-stressed condition. *J. Environ. Manag.* **2019**, *241*, 418–426. [CrossRef]
68. Ziganshina, E.E.; Belostotskiy, D.E.; Bulynina, S.S.; Ziganshin, A.M. Influence of Granular Activated Carbon on Anaerobic Co-Digestion of Sugar Beet Pulp and Distillers Grains with Solubles. *Processes* **2020**, *8*, 1226. [CrossRef]
69. Wang, Z.; Wang, T.; Si, B.; Watson, J.; Zhang, Y. Accelerating anaerobic digestion for methane production: Potential role of direct interspecies electron transfer. *Renew. Sustain. Energy Rev.* **2021**, *145*, 111069. [CrossRef]
70. Geissinger, O.; Herlemann, D.P.R.; Mörschel, E.; Maier, U.G.; Brune, A. The ultramicrobacterium "*Elusimicrobium minutum*" gen. nov., sp. nov., the first cultivated representative of the termite group 1 phylum. *Appl. Environ. Microbiol.* **2009**, *75*, 2831–2840. [CrossRef]
71. Zheng, H.; Dietrich, C.; Radek, R.; Brune, A. *Endomicrobium proavitum*, the first isolate of *Endomicrobia* class. nov. (phylum *Elusimicrobia*)—An ultramicrobacterium with an unusual cell cycle that fixes nitrogen with a Group IV nitrogenase. *Environ. Microbiol.* **2016**, *18*, 191–204. [CrossRef]
72. Hillesland, K.L.; Stahl, D.A. Rapid evolution of stability and productivity at the origin of a microbial mutualism. *Proc. Natl. Acad. Sci. USA* **2010**, *107*, 2124–2129. [CrossRef]
73. Detman, A.; Mielecki, D.; Pleśniak, L.; Bucha, M.; Janiga, M.; Matyasik, I.; Chojnacka, A.; Jędrysek, M.O.; Blaszczyk, M.K.; Sikora, A. Methane-yielding microbial communities processing lactate-rich substrates: A piece of the anaerobic digestion puzzle. *Biotechnol. Biofuels* **2018**, *11*, 116. [CrossRef]
74. Cotta, M.; Forster, R. The Family Lachnospiraceae, Including the Genera *Butyrivibrio*, *Lachnospira* and *Roseburia*. In *The Prokaryotes*; Dworkin, M., Falkow, S., Rosenberg, E., Schleifer, K.H., Stackebrandt, E., Eds.; Springer: New York, NY, USA, 2006; pp. 1002–1021.
75. Gagen, E.J.; Wang, J.; Padmanabha, J.; Liu, J.; Carvalho, I.P.C.; Liu, J.; Webb, R.I.; Al Jassim, R.; Morrison, M.; Denman, S.E.; et al. Investigation of a new acetogen isolated from an enrichment of the tammar wallaby forestomach. *BMC Microbiol.* **2014**, *14*, 314. [CrossRef] [PubMed]
76. Hung, C.H.; Chang, Y.T.; Chang, Y.J. Roles of microorganisms other than *Clostridium* and *Enterobacter* in anaerobic fermentative biohydrogen production systems—A review. *Bioresour. Technol.* **2011**, *102*, 8437–8444. [CrossRef] [PubMed]
77. Kim, T.G.; Yun, J.; Cho, K.S. The close relation between *Lactococcus* and *Methanosaeta* is a keystone for stable methane production from molasses wastewater in a UASB reactor. *Appl. Microbiol. Biotechnol.* **2015**, *99*, 8271–8283. [CrossRef]
78. Nesbø, C.L.; Bradnan, D.M.; Adebusuyi, A.; Dlutek, M.; Petrus, A.K.; Foght, J.; Doolittle, W.F.; Noll, K.M. *Mesotoga prima* gen. nov., sp. nov., the first described mesophilic species of the *Thermotogales*. *Extremophiles* **2012**, *16*, 387–393. [CrossRef] [PubMed]
79. Honda, T.; Fujita, T.; Tonouchi, A. *Aminivibrio pyruvatiphilus* gen. nov., sp. nov., an anaerobic, amino-acid-degrading bacterium from soil of a Japanese rice field. *Int. J. Syst. Evol. Microbiol.* **2013**, *63*, 3679–3686. [CrossRef] [PubMed]
80. Kuroda, K.; Nakajima, M.; Nakai, R.; Hirakata, Y.; Kagemasa, S.; Kubota, K.; Noguchi, T.Q.P.; Yamamoto, K.; Satoh, H.; Nobu, M.K.; et al. Microscopic and metatranscriptomic analyses revealed unique cross-domain symbiosis between *Candidatus* Patescibacteria/candidate phyla radiation (CPR) and methanogenic archaea in anaerobic ecosystems. *bioRxiv* **2023**. [CrossRef]
81. Barcelos, S.T.V.; Ferreira, I.F.L.; Costa, R.B.; Magalhães Filho, F.J.C.; Ribeiro, A.A.; Cereda, M.P. Startup of UASB reactor with limestone fixed bed operating in the thermophilic range using vinasse as substrate. *Renew. Energy* **2022**, *196*, 610–616. [CrossRef]
82. Anzola-Rojas, M.P.; Fuess, L.T.; Zaiat, M. Specific Organic Loading Rate Control for Improving Fermentative Hydrogen Production. *Fermentation* **2024**, *10*, 213. [CrossRef]
83. Borges, A.V.; Fuess, L.T.; Takeda, P.Y.; Rogeri, R.C.; Saia, F.T.; Gregoracci, G.B.; Damianovic, M.H.R.Z. Efficient Sulfidogenesis in Mesophilic Fermentation of Sugarcane Vinasse: Can Granular Sludge Outperform Natural Fermentation as Source of Inoculum? Available at SSRN, 2024. Available online: https://ssrn.com/abstract=4772239 (accessed on 20 April 2024).
84. Kapp, H. Sludge with a High Solids Content. Stuttgart Reports for Urban Water Management. Oldenbourg Verlag: Munich, Germany, 1984; Volume 86, p. 300.
85. Buchanan, I.D.; Nicell, J.A. Model development for horseradish peroxidase catalyzed removal of aqueous phenol. *Biotechnol. Bioeng.* **1997**, *54*, 251–261. [CrossRef]
86. Dubois, M.; Gilles, K.A.; Hamilton, J.K.; Rebers, P.A.; Smith, F. Colorimetric methods for determination of sugar and related substance. *Anal. Chem.* **1956**, *28*, 350–356. [CrossRef]
87. Taylor, K.A.C.C. A simple colorimetric assay for muramic acid and lactic acid. *Appl. Biochem. Biotechnol.* **1996**, *56*, 49–58. [CrossRef]
88. Adorno, M.A.T.; Hirasawa, J.S.; Varesche, M.B.A. Development and validation of two methods to quantify volatile acids (C2-C6) by GC/FID: Headspace (automatic and manual) and liquid-liquid extraction (LLE). *Am. J. Anal. Chem.* **2014**, *5*, 406–414. [CrossRef]

89. Lebrero, R.; Toledo-Cervantes, A.; Muñoz, R.; Del Nery, V.; Foresti, E. Biogas upgrading from vinasse digesters: A comparison between an anoxic biotrickling filter and an algal-bacterial photobioreactor. *J. Chem. Technol. Biotechnol.* **2016**, *91*, 2488–2495. [CrossRef]
90. Caporaso, J.G.; Lauber, C.L.; Walters, W.A.; Berg-Lyons, D.; Lozupone, C.A.; Turnbaugh, P.J.; Fierer, N.; Knight, R. Global patterns of 16S rRNA diversity at a depth of millions of sequences per sample. *Proc. Natl. Acad. Sci. USA* **2011**, *108*, 4516–4522. [CrossRef] [PubMed]
91. R Core Team. *R: A Language and Environment for Statistical Computing*; R Foundation for Statistical Computing: Vienna, Austria, 2020.
92. Pages, H.; Aboyoun, P.; Gentleman, R.; DebRoy, S. Biostrings: Efficient Manipulation of Biological String; R Package Version 2.64.1. Available online: https://s3.jcloud.sjtu.edu.cn/899a892efef34b1b944a19981040f55b-oss01/bioconductor/3.15/bioc/manuals/Biostrings/man/Biostrings.pdf (accessed on 13 October 2022).
93. Martin, M. Cutadapt removes adapter sequences from high-throughput sequencing reads. *EMBnet. J.* **2011**, *17*, 10–12. [CrossRef]
94. Callahan, B.J.; McMurdie, P.J.; Rosen, M.J.; Han, A.W.; Johnson, A.J.; Holmes, S.P. DADA2: High-resolution sample inference from Illumina amplicon data. *Nat. Methods* **2016**, *13*, 581–583. [CrossRef] [PubMed]
95. Cox, M.P.; Peterson, D.A.; Biggs, P.J. SolexaQA: At-a-glance quality assessment of Illumina second-generation sequencing data. *BMC Bioinform.* **2010**, *11*, 485. [CrossRef]
96. Wright, E.S. Using DECIPHER V2.0 to Analyze Big Biological Sequence Data in R. *R J.* **2016**, *8*, 352–359. [CrossRef]
97. Quast, C.; Pruesse, E.; Yilmaz, P.; Gerken, J.; Schweer, T.; Yarza, P.; Peplies, J.; Glöckner, F.O. The SILVA ribosomal RNA gene database project: Improved data processing and web-based tools. *Nucleic Acids Res.* **2013**, *41*, D590–D596. [CrossRef]
98. Piffer, M.A.; Oliveira, C.A.; Bovio-Winkler, P.; Eng, F.; Etchebehere, C.; Zaiat, M.; Nascimento, C.A.O.; Fuess, L.T. Sulfate- and pH-driven metabolic flexibility in sugarcane vinasse dark fermentation stimulates biohydrogen evolution, sulfidogenesis or homoacetogenesis. *Int. J. Hydrogen Energy* **2022**, *47*, 31202–31222. [CrossRef]